



**HAL**  
open science

# Stability and Reachability analysis for a controlled heterogeneous population of cells

Cécile Carrère, Hasnaa Zidani

► **To cite this version:**

Cécile Carrère, Hasnaa Zidani. Stability and Reachability analysis for a controlled heterogeneous population of cells. *Optimal Control Applications and Methods*, 2020, 41, pp.1678-1704. hal-01978686v2

**HAL Id: hal-01978686**

**<https://hal.science/hal-01978686v2>**

Submitted on 7 May 2020

**HAL** is a multi-disciplinary open access archive for the deposit and dissemination of scientific research documents, whether they are published or not. The documents may come from teaching and research institutions in France or abroad, or from public or private research centers.

L'archive ouverte pluridisciplinaire **HAL**, est destinée au dépôt et à la diffusion de documents scientifiques de niveau recherche, publiés ou non, émanant des établissements d'enseignement et de recherche français ou étrangers, des laboratoires publics ou privés.

## ARTICLE TYPE

# Stability and Reachability analysis for a controlled heterogeneous population of cells.

Cécile Carrère<sup>1</sup> | Hasnaa Zidani<sup>2</sup>

<sup>1</sup>Instituto Gulbenkian de Ciência, Fundação Callouste Gulbenkian, Oeiras, Portugal

<sup>2</sup>Unité de Mathématiques Appliquées, ENSTA ParisTech, Saclay, France

**Correspondence**

Email: cmcarrere@gulbenkian.pt

This paper is devoted to the study of a controlled population of cells. The modelling of the problem leads to a mathematical formulation of stability and reachability properties of some controlled systems under uncertainties. We use the Hamilton-Jacobi (HJ) approach to address these problems and to design a numerical method that we analyse on several numerical simulations.

**KEYWORDS:**

Non-linear optimal control; Dynamical programming; Applications to chemotherapy; Reachability analysis

## 1 | INTRODUCTION

The treatment of cancers with cytotoxic chemotherapies often encounters two major pitfalls: the side toxicity of the drugs on healthy cells and organs, and the emergence of resistance to the treatment. This resistance can occur because of an initial genomic heterogeneity of the tumour: in its early stages, it contains several distinct populations of cells, that differ from one another because of successive mutations<sup>1</sup>. If one of these lineages is resistant to the first line of treatment, then using strong doses of drug, as it is done in many classical protocols, kills all sensitive cells, and lets this resistant lineage grow without control. It is thus important to take into account cancer heterogeneity before starting a treatment. Mathematical modelling can, in this framework, give guidelines on how to treat such tumours.

For example,<sup>2,3</sup> study the growth and treatment of heterogeneous tumours, and determine optimal dosages of drugs for fixed time injections. The treatment protocol is there considered as instantaneous injections of drugs. We will work here in a framework of continuous treatment. In<sup>4</sup>, an ODE model of heterogeneous tumour growth is studied under continuous treatment. The optimal control theory is used to give necessary conditions on optimal protocols, in order to reduce the tumour volume while preserving its heterogeneity. We refer the reader to<sup>5,4,6,7</sup> for different models of tumour growth, presented and studied in the framework of optimal control theory.

In this paper, we will consider a model for heterogeneous tumour growth, with interactions between two cancerous cells populations:  $s$  which is sensitive to the treatment, and  $r$  which is resistant to it. The biological model is an *in vitro* experiment, with both lineages developing in a Petri dish, so that no other cells intervene in their evolution. It has been already considered in<sup>8</sup>, where an optimal treatment is characterized to treat heterogeneous tumours. This objective is satisfactory for experiments on *in vitro* tumors, but might not be adequate for medical applications with longer time objectives.

The main goal of the present work is to maintain permanently the tumour size under a certain threshold, defined by medical considerations, under which the tumour is considered benign. When this objective cannot be satisfied (for instance, if the initial tumour is already bigger than the designed threshold), we would like to find a good strategy to lower the tumour volume, in such a way that we will then be able to maintain it under the size threshold. These problems will be referred as stability or reachability problems. We will formulate these objectives as control problems that we will solve in the framework of Hamilton-Jacobi (HJ) equations.

An important problem arising from biological applications is the influence of uncertainties. For example, since several cytotoxic drugs target cells during their dividing phase, the drug efficiency may greatly differ depending on the tumour composition at the time of injection. The Hamilton-Jacobi framework is suitable to consider uncertainties as an opponent player, thus adjusting the optimal strategies to varying parameters.

Hamilton-Jacobi theory has been investigated, for stability and reachability problems, in many works. We refer to<sup>9,10,11,12,13,14,15,16</sup> and the references therein. In particular, let us also mention the works<sup>17</sup> where Hamilton-Jacobi framework is considered to take into account uncertainties in the case of collision avoidance for unmanned vehicles. In that paper, the uncertainty is the trajectory of another vehicle.

Recall that Hamilton-Jacobi equations characterise the value function associated to the control problem. Once this value function is computed numerically, a reconstruction algorithm can be used to get the optimal strategies for stability or for reachability. In this paper, we consider a reconstruction algorithm for control problems in presence of state constraints. We prove the convergence of this algorithm and we show with several numerical simulations the relevance of our approach.

This article is organized as follows. Section 2 presents the different models, objectives and constraints that will be considered in this paper. Section 3 is devoted to the mathematical analysis. In this section, a Hamilton-Jacobi approach is introduced to characterize some reachability sets. In section 4, we analyse some trajectory reconstruction algorithms. Finally, section 5 presents and analyses some numerical simulations.

## 2 | MATHEMATICAL FORMULATION OF THE PROBLEM

We present here some notations that will be used throughout this paper. We will denote by  $|\cdot|$  the Euclidean norm and by  $\langle \cdot, \cdot \rangle$  the Euclidean inner product on  $\mathbb{R}^N$  (for any  $N \geq 1$ ). The notation  $\mathbb{B}$  stands for the unit open ball  $\{x \in \mathbb{R}^N : |x| < 1\}$  and  $\mathbb{B}(x, r) := x + r\mathbb{B}$  for any  $x \in \mathbb{R}^N$  and  $r > 0$ .

For every set  $\mathcal{M} \subseteq \mathbb{R}^N$ ,  $\overset{\circ}{\mathcal{M}}$ ,  $\overline{\mathcal{M}}$  and  $\partial\mathcal{M}$  denote its interior, closure and boundary, respectively. The distance function to  $\mathcal{M}$  is  $\text{dist}(x, \mathcal{M}) = \inf\{|x - y| : y \in \mathcal{M}\}$ .

For any  $M > 0$ , the set  $L^1(0, +\infty; e^{-Mt} dt)$  is the set of functions  $f : [0, +\infty) \rightarrow \mathbb{R}$  such that  $\int_0^{+\infty} |f(t)|e^{-Mt} dt$  is finite:  $|f|$  is integrable for the measure  $e^{-Mt} dt$ . The set  $W^{1,1}(0, +\infty; e^{-Mt} dt)$  is the set of functions  $f \in L^1(0, +\infty; e^{-Mt} dt)$  such that their derivative is also in  $L^1(0, +\infty; e^{-Mt} dt)$ .

We consider the following controlled differential system :

$$\dot{y}(t) = f_0(y(t), \alpha(t)) + f_1(y(t), \alpha(t))u(t), \quad (1)$$

where  $u$  is the control,  $y$  the vector of state variables ( $y(t) \in \mathbb{R}^n$ , with  $n = 2$  or  $3$  depending on the problem we consider), and  $\alpha(t)$  a vector of  $m$  parameters that can change over time  $t$ , representing the uncertainties. We consider only measurable controls taking value between 0 and a certain  $U_{max} > 0$ ; in other words,

$$u \in \mathcal{U} := \{u : \mathbb{R}^+ \rightarrow \mathbb{R} \text{ is measurable, } u(t) \in [0, U_{max}] \text{ a.e.}\}.$$

We also consider that the uncertainties are measurable functions taking values in a given compact subset  $A$  of  $\mathbb{R}^m$  (with  $(m \geq 1)$ ):

$$\alpha \in \mathcal{A} := \{\alpha : \mathbb{R}^+ \rightarrow \mathbb{R}^m \text{ is measurable, } \alpha(t) \in A \text{ a.e.}\}$$

In all the sequel, we will consider models where the vector fields  $f_0 : \mathbb{R}^n \times \mathbb{R}^m \rightarrow \mathbb{R}^n$  and  $f_1 : \mathbb{R}^n \times \mathbb{R}^m \rightarrow \mathbb{R}^n$  satisfy the following assumption:

( $\mathbf{H}_f$ )  $f_0$  and  $f_1$  are continuous functions, and Lipschitz continuous with respect to the first variable uniformly with respect to the second variable: there exists a constant  $M_0 > 0$  such that:

$$|f_0(x, \alpha) - f_0(x', \alpha)| + |f_1(x, \alpha) - f_1(x', \alpha)| \leq M_0|x - x'| \quad \forall x, x' \in \mathbb{R}^n \text{ and } \forall \alpha \in A. \quad (2)$$

Under this assumption the functions  $f_0$  and  $f_1$  satisfy a linear growth: there exists a constant  $M_1 > 0$  such that:

$$|f_0(x, \alpha)| \leq M_1(1 + |x|) \quad \text{and} \quad |f_1(x, \alpha)| \leq M_1(1 + |x|) \quad \forall x \in \mathbb{R}^n \text{ and } \alpha \in A. \quad (3)$$

We will also use a function  $f$  that is defined as:

$$f(x, \alpha, u) = f_0(x, \alpha) + f_1(x, \alpha)u \quad \text{for } x \in \mathbb{R}^n, \alpha \in A, u \in [0, U_{max}].$$

Let  $x \in \mathbb{R}^n$ ,  $u \in \mathcal{U}$  be an admissible control and  $\alpha \in \mathcal{A}$  a perturbation. By a solution to (1) we mean an absolutely continuous function  $y(\cdot)$  that satisfies

$$y(t) = x + \int_0^t [f_0(y(s), \alpha(s)) + f_1(y(s), \alpha(s))u(s)]ds \quad \text{for all } t \geq 0.$$

By the Lipschitz continuity of  $f_0$ ,  $f_1$  and by their linear growth, the solution of (1) is uniquely determined by the control input  $u \in \mathcal{U}$ , the initial condition  $y(0) = x \in \mathbb{R}^n$  and the uncertainties  $\alpha \in \mathcal{A}$  and will be denoted by  $y_x^{\alpha, u}$ . Furthermore, the maximal solution is defined for all times. Note, that by the Gronwall Lemma, we have:

$$\begin{aligned} |y_x^{\alpha, u}(t)| &\leq (1 + |x|)e^{M_1 t} \quad t \geq 0, \\ |y_x^{\alpha, u}(t) - x| &\leq (1 + |x|)(e^{M_1 t} - 1) \quad t \geq 0, \\ |\dot{y}_x^{\alpha, u}(t)| &\leq M_1(1 + |x|)e^{M_1 t} \quad \text{a.e. } t > 0. \end{aligned}$$

Moreover, for any  $R > 0$ , there exists  $M_R > 0$  such that:

$$|y_x^{\alpha, u}(t) - y_{x'}^{\alpha, u}(t)| \leq M_R |x - x'| e^{M_0 t} \quad \forall x, x' \in \mathbb{B}(0, R).$$

For any  $x \in \mathbb{R}^n$ , we denote by  $S(x)$  the set of all solutions  $y_x^{\alpha, u}$ , on  $[0, +\infty[$ , of equation (1) associated to  $\alpha \in \mathcal{A}$  and  $u \in \mathcal{U}$  and with the initial condition  $x$ :

$$S(x) = \{y_x^{\alpha, u} \in W^{1,1}(0, +\infty, e^{-M_0 t}), \alpha \in \mathcal{A}, u \in \mathcal{U}\}.$$

In the control problems that we will consider, the control input  $u$  will have to adapt to uncertainties  $\alpha$ . In this context, we consider a differential game with two players, one can act by choosing the control  $\alpha$  and the other one can respond by choosing the function  $u$ . Following the work of<sup>18</sup>, we use the notion of strategies  $u : \alpha \mapsto u[\alpha]$ , and since we cannot predict the fluctuations of the parameters we consider the set of all non-anticipative strategies  $\Upsilon$  given as:

$$\begin{aligned} \Upsilon := \{ &u : \mathcal{A} \rightarrow \mathcal{U} / \forall (\alpha, \alpha') \in \mathcal{A} \text{ and } \forall t \geq 0, \\ &(\alpha(\tau) = \alpha'(\tau) \forall \tau \in [0, t]) \Rightarrow (u[\alpha](\tau) = u[\alpha'](\tau) \forall \tau \in [0, t]) \}. \end{aligned}$$

## 2.1 | Two models for heterogeneous tumour growth

The first model that will be considered in this paper, has been presented and studied in<sup>8</sup>. It represents the growth of two populations of cells in a Petri dish in competition for nutrients:  $s$  is the population sensitive to the treatment  $u$ , and  $r$  the population resistant to it. They are fairly similar, so their division rate for small populations  $\rho$  is identical. They compete for food and space with a logistic growth rate, which is represented by the total remaining space  $K - s(t) - mr(t)$ ,  $K$  being the size of the Petri dish and  $m$  the size ratio between sensitive and resistant cells. Moreover, interspecies competition is stronger on resistant than on sensitive cells, which is represented by a supplementary competition term  $\beta s(t)r(t)$ . We suppose that no mutations occur during the time of our study. Finally, the treatment only has an influence on the sensitive population.

$$\begin{cases} \frac{ds}{dt}(t) = \rho s(t) \left(1 - \frac{s(t) + mr(t)}{K}\right) - \gamma(t)s(t)u(t), \\ \frac{dr}{dt}(t) = \rho r(t) \left(1 - \frac{s(t) + mr(t)}{K}\right) - \beta(t)s(t)r(t). \end{cases} \quad (\text{M1})$$

This model includes some uncertainties  $\alpha(t) = (\gamma(t), \beta(t))$  on the drug efficiency and on the interspecies competition. We suppose throughout the paper that these uncertainties take values in a set  $A$  that has the following form

$$\alpha(t) \in A := [\gamma_{\min}, \gamma_{\max}] \times [\beta_{\min}, \beta_{\max}],$$

where the parameters  $\gamma_{\max} \geq \gamma_{\min} > 0$  and  $\beta_{\max} \geq \beta_{\min} > 0$  are given. The values that will be used in the numerical simulations are summed up in section 5, Table 1.

One can show easily that the set  $\mathcal{K} := \{(s, r) \in \mathbb{R}^2 / s \geq 0, r \geq 0 \text{ and } s + mr \leq K\}$  is invariant under the action of system (M1), whichever  $\alpha \in \mathcal{A}$  and  $u \in \mathcal{U}$  are. This is consistent with the fact that  $K$  represents the total space in the Petri dish, thus it is a bound on the size of the *in vitro* tumour.

*Remark 1.* Note that the dynamics function doesn't satisfy the Lipschitz continuity of assumption  $(\mathbf{H}_f)$ . However, since we are interested in system (M1) in  $\mathcal{K}$ , we can modify  $f_0$  and  $f_1$  outside of  $\mathcal{K}$  such that for a certain  $R > \max(K, K/m)$ ,  $|y| > R$  implies  $f_0(\alpha, y) = f_1(\alpha, y) = 0$  for any  $\alpha$ , then  $f_0$  and  $f_1$  are Lipschitz continuous on  $\mathbb{R}^2 \times \mathbb{R}^2$ .

In our simulations, we will consider the case where  $\gamma_{\min} U_{\max} > \rho$ , meaning that we have access to relatively large doses of treatment.

Limiting the drug dosage to a maximal value  $U_{\max}$  is important, but the cumulated dose of treatment over a period of time should also be kept under a certain threshold. Otherwise, cumulated effects on the patient global health can be very harmful<sup>19</sup>. A first solution to take this toxicity into account is to set the following condition: for any  $t \geq 0$ , we impose that:

$$\int_t^{t+\tau} u(s) ds \leq D_{\max} \quad (4)$$

where  $\tau$  is a typical time of treatment, and  $D_{\max}$  the maximal quantity, or dose, of treatment to be delivered during time  $\tau$ . This condition gives rise to a delayed system of equations. This proves very difficult to control, both theoretically and numerically, for the problems we are about to define. But since the necessity of (4) comes from a biological interpretation, one can transform this condition by adding a virtual global health indicator, which will keep track of the toxicity. We thus propose the following model:

$$\begin{cases} \frac{ds}{dt}(t) = \rho s(t) \left(1 - \frac{s(t)+mr(t)}{K}\right) - \gamma(t)s(t)u(t) \\ \frac{dr}{dt}(t) = \rho r(t) \left(1 - \frac{s(t)+mr(t)}{K}\right) - \beta(t)s(t)r(t) \\ \frac{dw}{dt}(t) = \rho_w - \mu w(t) - \nu w(t) \max(0, u(t) - u_{\text{tox}}). \end{cases} \quad (\text{M2})$$

This model is inspired by<sup>20</sup>, in which the state variable  $w$  is a white blood cells count. The new state variable  $w$  represents a virtual global health indicator, that is renewed at a constant rate  $\rho_w$ , evacuated from the system at rate  $\mu w$ , and destroyed by drug doses larger than the threshold  $u_{\text{tox}} > 0$ . The set

$$\mathcal{K}' := \{(s, r, w) \in \mathbb{R}^3 / s \geq 0, r \geq 0, w \geq 0, s + mr \leq K \text{ and } w \leq \rho_w / \mu\}$$

is invariant under action of system (M2). As mentioned in Remark 1, the dynamics can be changed in adequate way outside of  $\mathcal{K}'$  such that it fits assumption  $(\mathbf{H}_f)$ .

Note that in (M2), the indicator  $w$  does not interact with sensitive or resistant cancerous cells. Indeed, we are still considering cancerous cells cultivated *in vitro* without any other population: the state variable  $w$  only serves as a way to limit drug usage, by imposing for example  $w(t) \geq w_{\min}$  for any  $t \geq 0$ .

In Section 5, we will present numerical simulations of the problem ; the values chosen for the different parameters are listed in Table 1.

## 2.2 | Objective functions and state constraints

From now on, we will consider two control problems. Both problems involve the tumour size, that we define as:

$$\phi : y = (s, r) \mapsto s + mr.$$

For the simplicity of notations, even when we consider the model (M2) where the state variable is  $y = (s, r, w) \in \mathbb{R}^3$ , we will still denote  $\phi(y) = s + mr$ .

Now, we can state the two problems that will be considered in this paper. The first one is a stability problem.

**Problem 1 (Stability).** Let  $Q > 0$  be such that  $Q < K$ . Given  $x_0 \in \mathbb{R}^n$ , does there exist a strategy  $u \in \mathcal{Y}$  such that for any perturbation  $\alpha \in \mathcal{A}$ ,

$$\forall t \geq 0, \phi(y_{x_0}^{\alpha, u[\alpha]}(t)) \leq Q.$$

In other words, given a threshold in tumour size  $Q$ , can we find a control strategy such that the tumour size never exceeds this threshold?

The second problem that will be analysed in this paper is a reachability problem.

**Problem 2 (Reachability).** Let  $Q > 0$  be such that  $Q \leq K$ , and let  $T > 0$ . For  $x_0 \in \mathbb{R}^n$ , does there exist a strategy  $u \in \mathcal{Y}$  and a minimal time  $\mathcal{T} \in [0, T]$  such that, for any perturbation  $\alpha \in \mathcal{A}$ ,

$$\forall t \geq \mathcal{T}, \phi(y_{x_0}^{\alpha, u[\alpha]}(t)) \leq Q.$$

In other words, given a certain time of treatment  $T$ , minimize the time  $\mathcal{T}$  at which the tumour size is stabilized under the threshold  $Q$ , without this time exceeding  $T$ .

The above two problems will be considered for models (M1) and (M2).

**State constraints** (Global health indicator). In both models (M1) and (M2), the functions  $s(\cdot)$  and  $r(\cdot)$  should take values respectively in  $[0, K]$  and  $[0, K/m]$ .

Furthermore, in the model (M2), the global health indicator system  $w(t)$  should remain above a certain threshold  $w_{\min}$ , at any time  $t$ :

$$\forall t \geq 0, w(t) \geq w_{\min}, \quad (5)$$

where  $w_{\min}$  is a given constant that satisfies  $\frac{\rho w}{\mu} > w_{\min}$ . One can also check from the dynamics of  $w$  that if  $w(0) \leq \frac{\rho w}{\mu}$ , then:

$$\forall t \geq 0, w(t) \leq \frac{\rho w}{\mu}.$$

### 3 | STABILITY AND REACHABILITY

We now describe the mathematical formulations that will be used to address Problems 1 and 2.

#### 3.1 | Definition of the stability kernel

Let  $\mathbb{T}$  be a subset of  $\mathbb{R}^n$ . We will call the stability kernel of  $\mathbb{T}$  under the dynamics (2.1) the set  $\mathcal{N}_{\mathbb{T}} \subset \mathbb{R}^n$  defined by:

$$\mathcal{N}_{\mathbb{T}} := \{x \in \mathbb{R}^n / \exists u \in \Upsilon, \forall \alpha \in \mathcal{A}, \forall t > 0, y_x^{\alpha, u}(\alpha)(t) \in \mathbb{T}\}.$$

It is the set of starting points for which there exists a strategy  $u \in \Upsilon$  that keeps the solution in  $\mathbb{T}$  for any time  $t \geq 0$  and for any perturbation  $\alpha \in \mathcal{A}$ .

Let us point out that the above definition of stability is identical to the notion of discriminating kernel analyzed in<sup>21</sup>. It is also related to the notion of viability under set-valued dynamics in the monograph<sup>22</sup>. Here, we prefer to call the set  $\mathcal{N}_{\mathbb{T}}$  a stability set because it will represent in our application the initial composition of the tumours that can be kept forever under a certain size threshold.

In our context as described in the previous section, and in order to answer the stability problem (Problem 1), we are lead to the question of determining the stability kernel for a set  $\mathbb{T}_Q$  that is defined, for a given threshold value  $Q \in (0, K)$  of the tumour size, as follows:

- In case of model (M1),

$$\mathbb{T}_Q := \{(s, r) \in \mathbb{R}^2 / s \geq 0, r \geq 0 \text{ and } s + mr \leq Q\}$$

- In case of model (M2),

$$\mathbb{T}_Q := \{(s, r, w) \in \mathbb{R}^3 / s \geq 0, r \geq 0, s + mr \leq Q, \text{ and } w \in [w_{\min}, \frac{\rho w}{\mu}]\}.$$

**Proposition 1.** For Model (M1), if  $Q > K(1 - \frac{\gamma_{\min}}{\gamma_{\max}} \frac{1}{1 + \rho/K\beta_{\min}})$ , then  $\mathcal{N}_{\mathbb{T}_Q}$  has a non empty interior. If  $Q \leq \frac{K}{1 + K\beta_{\min}/\rho}$  then  $\mathcal{N}_{\mathbb{T}_Q} = [0, Q] \times \{0\}$ .

*Proof.* The two assertions of this proposition come from phase plane analysis of System (M1).

Assume that  $Q > K(1 - \frac{\gamma_{\min}}{\gamma_{\max}} \frac{1}{1 + \rho/K\beta_{\min}})$ . In this case, consider the constant control  $u(t) \equiv u^0 = \frac{1}{\gamma_{\max}} \frac{K\beta_{\min}}{1 + K\beta_{\min}/\rho}$ . For any fixed  $\beta \in [\beta_{\min}, \beta_{\max}]$ , and any fixed  $\gamma \in [\gamma_{\min}, \gamma_{\max}]$ , one can check that the point  $(K(1 - \frac{\gamma}{\rho}u^0), 0)$  is stable and locally attractive in  $\mathbb{R}^2$  since  $K(1 - \frac{\gamma}{\rho}u^0) > \frac{K}{1 + K\beta_{\min}/\rho}$ . Thus the segment  $[K(1 - \frac{\gamma_{\max}}{\rho}u^0), K(1 - \frac{\gamma_{\min}}{\rho}u^0)] \times \{0\}$  is locally attractive in  $\mathbb{R}^2$  for any perturbation  $\alpha(t)$ . Thus there exists a neighbourhood of this segment embedded in  $\mathcal{N}_{\mathbb{T}_Q}$ , since  $K(1 - \frac{\gamma_{\min}}{\rho}u^0) \leq Q$ .

Now, consider the case  $Q \leq \frac{K}{1 + K\beta_{\min}/\rho}$ .

Under constant control  $u(t) \equiv \frac{\rho}{\gamma_{\max}}(1 - \frac{Q}{K})$ , for any  $s \in (0, Q]$  and any perturbation  $\alpha \in \mathcal{A}$ , we have  $y_{(s,0)}^{\alpha, u}(t) \in (0, Q]$  for all  $t \geq 0$ . Moreover,  $(0, 0)$  is stable under any treatment, thus  $[0, Q] \times \{0\} \subset \mathcal{N}_{\mathbb{T}_Q}$ . However, suppose that  $\beta(t) \equiv \beta_{\min}$ ; for any

$(s, r) \in \mathbb{T}_Q$  such that  $r > 0$ , we have  $\frac{dr}{dt}(t) \geq r\beta_{\min}(\frac{K}{1+K\beta_{\min}/\rho} - s) > 0$ . Thus any trajectory starting in  $\mathbb{T}_Q$  will leave it in a finite time.  $\square$

With similar arguments as in the above proof, it is possible to check that the statement of proposition 1 is still true for system (M2) as long as  $u_{\text{tox}} > \frac{\rho}{\gamma_{\min}}(1 - \frac{1}{1+K\beta_{\min}/\rho})$ .

As we are interested in controlling heterogeneous tumours (*i.e.* with  $r > 0$ ), we will consider in the sequel that  $Q > \frac{1}{1+K\beta_{\min}/\rho}$ .

### 3.2 | Level-set approach for stability problem

To characterize the stability kernel, we use a level-set approach and define a control problem and its value function whose 0-sub-level set coincides exactly with the stability kernel (see <sup>15,17</sup> and the references therein).

For this, we fix  $Q > \frac{1}{1+K\beta_{\max}/\rho}$  and define a bounded Lipschitz continuous function  $g_Q : \mathbb{R}^n \rightarrow \mathbb{R}^+$  such that

$$x \in \mathbb{T}_Q \iff g_Q(x) = 0.$$

A particular choice of  $g_Q$  could be:

$$g_Q(x) = \min(1, \text{dist}(x, \mathbb{T}_Q)).$$

Now, consider the following control problem parametrized by the initial position  $x \in \mathbb{R}^n$ :

$$(\mathcal{P}_x) \quad \min_{u \in \mathcal{Y}} \max_{\alpha \in \mathcal{A}} \int_0^{+\infty} e^{-\lambda t} g_Q(y_x^{\alpha, u}(t)) dt,$$

where  $\lambda > 0$  is a constant that will be chosen later. We consider also the value function (called also cost-to-go function) defined by:

$$V_Q(x) = \min(\mathcal{P}_x), \quad \forall x \in \mathbb{R}^n.$$

Before studying this control problem, let us first point out some straightforward remarks on the value function.

*Remark 2.* First,  $g_Q$  being bounded, the integral  $\int_0^{+\infty} e^{-\lambda t} g_Q(y_x^{\alpha, u}(t)) dt$  is well-defined for any  $\alpha \in \mathcal{A}$  and any  $u \in \mathcal{U}$ . Also, because the function  $g_Q$  is bounded, the value function  $V_Q$  is also bounded.

Furthermore, it is not difficult to check that the stability kernel  $\mathcal{N}_{\mathbb{T}_Q}$  can be characterized as the 0-sub-level set of the function  $V_Q$ :

$$\mathcal{N}_{\mathbb{T}_Q} = \{x \in \mathbb{R}^n \mid V_Q(x) = 0\}.$$

In the sequel, we shall study the properties of the value function  $V_Q$  and show a way to get an efficient approximation on  $\mathcal{K}$  by solving an appropriate partial differential equation.

**Proposition 2.** The value function  $V_Q$  is Lipschitz continuous on  $\mathbb{R}^n$  if  $\lambda$  is large enough. Moreover, it satisfies the following dynamic programming principle:

$$\forall x \in \mathbb{R}^n, \forall h > 0, V_Q(x) = \min_{u \in \mathcal{Y}} \max_{\alpha \in \mathcal{A}} \left( \int_0^h e^{-\lambda t} g_Q(y_x^{\alpha, u}(t)) dt + e^{-\lambda h} V_Q(y_x^{\alpha, u}(h)) \right). \quad (6)$$

*Proof.* Because  $f$  is Lipschitz continuous on  $\mathbb{R}^n$  for problems (M1) and (M2), according to the Gronwall lemma, for any  $x, x' \in \mathbb{R}^n$ , any  $t \geq 0$ , any  $\alpha \in \mathcal{A}$  and any  $u \in \mathcal{U}$ ,

$$|y_x^{\alpha, u}(t) - y_{x'}^{\alpha, u}(t)| \leq e^{M_0 t} |x - x'|.$$

Furthermore, function  $g_Q$  is 1-Lipschitz continuous, thus for  $x, x' \in \mathbb{R}^n$ , we have:

$$\begin{aligned} |V_Q(x) - V_Q(x')| &= \left| \inf_{u \in Y} \max_{\alpha \in A} \int_0^{+\infty} e^{-\lambda t} g_Q(y_x^{\alpha, u[\alpha]}(t)) dt - \inf_{u \in Y} \max_{\alpha \in A} \int_0^{+\infty} e^{-\lambda t} g_Q(y_{x'}^{\alpha, u[\alpha]}(t)) dt \right| \\ &\leq \sup_{u \in Y} \max_{\alpha \in A} \int_0^{+\infty} e^{-\lambda t} |g_Q(y_x^{\alpha, u[\alpha]}(t)) - g_Q(y_{x'}^{\alpha, u[\alpha]}(t))| dt \\ &\leq \int_0^{+\infty} e^{-\lambda t} e^{M_0 t} |x - x'| dt. \end{aligned}$$

If we choose  $\lambda > M_0$ , then the function  $V_Q$  is Lipschitz continuous.

The proof of the dynamical programming principle comes from classical arguments (see<sup>23</sup> for example).  $\square$

From (6), one can show that  $V_Q$  satisfies a Hamilton-Jacobi equation:

**Theorem 1.** For any  $\lambda > M_0$ , the value function  $V_Q$  is the unique viscosity solution of the Hamilton-Jacobi equation:

$$\lambda V_Q + H(x, D_x V_Q) - g_Q(x) = 0, \quad x \in \mathbb{R}^d, \quad (7)$$

where  $D_x V_Q$  represents the derivative of  $V_Q$  (in the viscosity sense), and the Hamiltonian  $H : \mathbb{R}^n \times \mathbb{R}^n \rightarrow \mathbb{R}$  is defined by:

$$H(x, p) := \min_{\alpha \in A} \max_{u \in [0, U_{\max}]} \langle -f(x, \alpha, u), p \rangle.$$

This theorem can be obtained by using classical arguments in viscosity theory<sup>24,23</sup>.

We note that the expression of the hamiltonian  $H$  can be given in a more explicit form for the different models we are considering in this paper:

**For model (M1),**

the hamiltonian is:

$$\begin{aligned} H((s, r), p) &= -p_1 \rho s \left(1 - \frac{s + mr}{K}\right) - p_2 \rho r \left(1 - \frac{s + mr}{K}\right) + \min(p_2 \beta_{\min} sr, p_2 \beta_{\max} sr) \\ &\quad + \max(0, \gamma_{\min} s u_{\max} p_1). \end{aligned}$$

**For model (M2),**

the hamiltonian is:

$$\begin{aligned} H((s, r, w), p) &= -p_1 \rho s \left(1 - \frac{s + mr}{K}\right) - p_2 \rho r \left(1 - \frac{s + mr}{K}\right) - p_3 (\rho w - \mu w) \\ &\quad + \min(p_2 \beta_{\min} sr, p_2 \beta_{\max} sr) \\ &\quad + \max(0, \gamma_{\min} s u_{\text{tox}} p_1, \gamma_{\min} s U_{\max} p_1 + \mu w (U_{\max} - u_{\text{tox}}) p_3). \end{aligned}$$

These expressions will be useful for the numerical implementation purposes in the approximation of the HJ equation.

### 3.3 | Minimum time function - Reachability problem

We now move to the problem of reachability (Problem 2). Here, we assume that  $\mathcal{N}_{\mathbb{T}_Q}$  is known (or an approximation of  $\mathcal{N}_{\mathbb{T}_Q}$  is given). Then, we are interested in the set of initial positions from where there exists an admissible trajectory that can reach  $\mathcal{N}_{\mathbb{T}_Q}$  in a finite time horizon  $T > 0$  while remaining in a given domain;  $\mathcal{D} := [0, K] \times [0, K/m]$  for model (M1), and  $\mathcal{D} := [0, K] \times [0, K/m] \times [w_{\min}, \frac{\rho w}{\mu}]$  for model (M2). Therefore, the capture basin is defined as:

$$\mathcal{R}(T) := \{x \in \mathbb{R}^n \mid \exists u \in Y, \forall \alpha \in A, y_x^{\alpha, u[\alpha]}(T) \in \mathcal{N}_{\mathbb{T}_Q} \text{ and } y_x^{\alpha, u[\alpha]}(s) \in \mathcal{D} \forall s \in [0, T]\}.$$

An illustration of  $\mathcal{N}_{\mathbb{T}_Q}$  and some trajectories reaching it are presented in Figure 1. In this figure, the filled region represents the set  $\mathcal{N}_{\mathbb{T}_Q}$ . Starting from the points  $A$  or  $B$ , it is possible to find admissible trajectories that can reach  $\mathcal{N}_{\mathbb{T}_Q}$  in a finite horizon  $T$ . So both points  $A$  and  $B$  are in the capture basin (represented in the figure as the set surrounded by the dashed line).



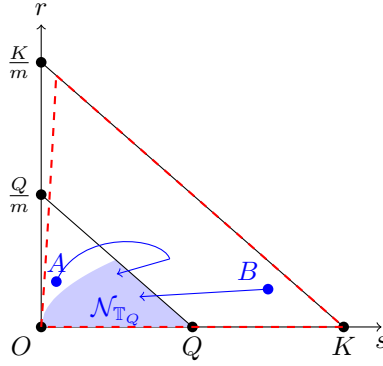


**FIGURE 1** Illustration of the sets  $\mathcal{N}_{T_Q}$  (filled region) and  $\mathcal{R}(T)$  (set surrounded by the dashed line).

Notice that for some  $x \in \mathbb{R}^n$ , it may not be possible to get to the stability kernel  $\mathcal{N}_{T_Q}$  in a finite time. For example, if  $x = (0, K/m)$ , then for any  $t \geq 0$ , any  $u \in \mathcal{U}$  and any  $\alpha \in \mathcal{A}$ , we have  $y_x^{\alpha, u}(t) = (0, K/m)$ . Thus, if  $Q < K$ , whatever control is chosen, the trajectory will never enter  $\mathcal{N}_{T_Q}$ .

Here again, we will follow some ideas investigated by<sup>25,26,27,15</sup> and use a level-set approach to define the capture basin  $\mathcal{R}(T)$  at time  $T$ .

First, we introduce the function  $g : \mathbb{R}^n \rightarrow \mathbb{R}$  that is the oriented distance to the set  $D$ :

$$g_w(x) := \begin{cases} \text{dist}(x, \partial D) & \text{if } x \in \mathbb{R}^n \setminus D, \\ -\text{dist}(x, \partial D) & \text{if } x \in D. \end{cases}$$

Now consider the control problem and its value function  $W$  defined, for every  $x \in \mathbb{R}^n$  and  $t \in [0, T]$ , by:

$$W(x, t) := \min_{u \in \mathcal{Y}} \max_{\alpha \in \mathcal{A}} \left\{ \max \left( \max_{0 \leq \tau \leq t} g_w(y_x^{\alpha, u}(\tau)), V_Q(y_x^{\alpha, u}(t)) \right) \right\}.$$

According to<sup>15</sup>, for  $T > 0$ , the capture basin is given by:

$$\mathcal{R}(T) = \{x \in \mathbb{R}^n \mid W(x, T) \leq 0\}.$$

Moreover, the minimum time,  $\mathcal{T}(x)$ , for a starting position  $x \in \mathbb{R}^n$  to reach the target  $\mathcal{N}_{T_Q}$  (before time  $T$ ) is given by:

$$\mathcal{T}(x) = \min\{t \in [0, T] \mid W(x, t) \leq 0\}. \quad (8)$$

Besides, as it has been shown in<sup>15</sup>, the value function  $W$  satisfies the following dynamical programming principle for every  $x \in \mathbb{R}^n$ , for every  $t \in [0, T]$  and  $h \in [0, T - t]$ :

$$W(x, t + h) = \min_{u \in \mathcal{Y}} \max_{\alpha \in \mathcal{A}} \left( \max \left( \max_{0 \leq \tau \leq h} g_w(y_x^{\alpha, u}(\tau)), W(y_x^{\alpha, u}(h), t) \right) \right),$$

and  $W$  is the unique viscosity solution to the following Hamilton-Jacobi-Bellman equation:

$$\min \left( \partial_t W(x, t) + H(x, \nabla D_x(x, t)), W(x, t) - g_w(x) \right) = 0 \quad \text{for } x \in \mathbb{R}^n, t \in (0, T], \quad (9a)$$

$$W(x, 0) = V_Q(x) \quad \text{for } x \in \mathbb{R}^n, \quad (9b)$$

where  $\partial_t W(x, t)$  and  $D_x W(x, t)$  are respectively the time derivative and the space derivative (in the sense of viscosity notion, see<sup>23</sup>).

## 4 | TRAJECTORIES RECONSTRUCTION

Once the value functions are constructed up to some error on a grid of calculations, we want to deduce optimal controls for a starting position  $x_0$ .

## 4.1 | A trajectory staying in $\mathcal{N}_{\mathbb{T}_Q}$

Let  $f^h$  be a family of numerical approximations of  $f$ . We make the following assumption:

( $\mathbf{H}_{A1}$ ) for any  $R > 0$ , there exists  $\kappa_R > 0$  independant of  $h$  such that:

$$|f(x, \alpha, u) - f^h(x, \alpha, u)| \leq \kappa_R h \quad \forall |x| < R, \alpha \in A, u \in U$$

We will use an approximation scheme for the differential equation using  $f^h$ : an approximation of  $y_x^{\alpha, u}(t)$  with constant  $\alpha$  and  $u$  will be

$$\tilde{y} = x + h f^h(x, \alpha, u).$$

For example, the case of an Euler forward scheme corresponds to the choice  $f^h = f$ .

Now, for any  $h \in (0, 1)$  consider an approximation of  $V_Q$ , noted  $V_Q^h$ . We make the following assumption:

( $\mathbf{H}_{A2}$ ) For every  $h \in (0, 1)$ , there exists an approximation  $V_Q^h$  of  $V_Q$ , which satisfies:

$$E_h := \max_x |V_Q(x) - V_Q^h(x)|, \quad \frac{E_h}{h} \xrightarrow{h \rightarrow 0} 0.$$

*Remark 3.* The theory of approximation of viscosity solutions states that for a given time step size  $\tau$ , an approximation  $V_{Q, \tau}$  of  $V_Q$  can be computed with an error of order  $\sqrt{\tau}$ . This error is guaranteed under some stability assumptions linking the time and space mesh sizes (the so-called CFL condition). So to comply with the assumption ( $\mathbf{H}_{A2}$ ), one can consider the approximation  $V_Q^h = V_{Q, \tau(h)}$  where  $\tau(h) = h^k$  with  $k > 2$ . In this case,

$$\frac{E(h)}{h} = O\left(\frac{\sqrt{h^k}}{h}\right) = O\left(h^{\frac{k-2}{2}}\right) \xrightarrow{h \rightarrow 0} 0,$$

and assumption ( $\mathbf{H}_{A2}$ ) is satisfied.

Let  $h \in (0, 1)$  be a time step, and  $N_h \in \mathbb{N}$  a number of steps. The actual realization of the uncertainties  $\bar{\alpha}$  is known ; we will denote  $\alpha_k = \bar{\alpha}(kh)$  for simplicity. For any  $y \in \mathbb{R}^2$ , we define the trajectory reconstruction algorithm up to time  $T_h = N_h h$ , described in Algorithm 1.

---

### Algorithm 1 Stability

---

The starting point  $y$  and the uncertainties realization  $\bar{\alpha} = (\bar{\alpha}_k)_k$  are known.

*Initialization* Set  $y_0^h = y$ .

*Recursive definition of  $y_k^h$*  Suppose  $(y_\ell^h)$  is known for  $\ell = 0 \dots k-1$ . To determine  $y_k^h$ , we define an optimal control  $u_k^h$  such that:

$$u_k^h \in \operatorname{argmin}_{u \in U} V_Q^h(y_{k-1}^h + h f^h(y_{k-1}^h, \bar{\alpha}_k, u)) e^{-\lambda h} + \lambda h g_Q(y_{k-1}^h).$$

The new position is then defined by:

$$y_k^h = y_{k-1}^h + h f^h(y_{k-1}^h, \bar{\alpha}_k, u_k^h).$$

*Complete trajectory* We associate to the sequence of controls  $(u_k^h)_k$  the piecewise constant function  $\mathbf{u}^h(t) = u_k^h$  for  $t \in [kh, (k+1)h)$ , and an approximate trajectory  $\mathbf{y}^h$  defined on  $[0, +\infty)$  by:

$$\begin{cases} \dot{\mathbf{y}}^h(t) = f^h(y_k^h, \bar{\alpha}_k, u_k^h) & \text{for } t \in (kh, (k+1)h) \\ \mathbf{y}^h(kh) = y_k^h & \forall k \in \mathbb{N}, k \leq N_h \\ \dot{\mathbf{y}}^h(t) = f(\mathbf{y}(t), \bar{\alpha}, 0) & \forall t > T_h \end{cases}$$


---

Note that in general,  $y_{y_0}^{\bar{\alpha}, u^h} \neq \mathbf{y}^h$ . We shall show that any accumulation point  $\bar{\mathbf{y}}$  of  $(\mathbf{y}^h)_h$  is a trajectory realizing better than a minimum for the cost function  $V_Q$ : since  $\bar{\alpha}$  is an actual realization of the uncertainties, it might be "better than the worst".

**Theorem 2.** Let  $y \in \mathbb{R}^n$  and let  $(y_k^h)$  be the sequence defined by Algorithm1, under hypothesis ( $\mathbf{H}_f$ ) and assumptions ( $\mathbf{H}_{A1}$ ) - ( $\mathbf{H}_{A2}$ ). Suppose furthermore the following limits to hold true:

$$N_h h \xrightarrow{h \rightarrow 0} +\infty, \quad N_h h^2 \xrightarrow{h \rightarrow 0} 0, \quad N_h E_h \xrightarrow{h \rightarrow 0} 0. \quad (10)$$

Then the functions  $(\mathbf{y}^h)$  form a better than minimizing sequence in the following sense:

$$V_Q(y) \geq \limsup_{h \rightarrow 0} \int_0^{+\infty} e^{-\lambda t} g_Q(\mathbf{y}^h(t)) dt \quad (11)$$

Furthermore, the family  $(\mathbf{y}^h)$  has an accumulation point  $\mathbf{y}$  in  $W^{1,1}([0, +\infty), e^{-M_0 t})$ , and if  $V_Q(y) = 0$  then it is a viable trajectory, in the sense that:

$$\forall t \geq 0, \mathbf{y}(t) \in \mathcal{N}_{\mathbb{T}_Q}.$$

*Proof.* Let  $y \in \mathbb{R}^2$  and let  $(y_k^h)$  and  $(u_k^h)$  be the corresponding sequences constructed by Algorithm 1. One can show that there exists  $R > 0$  such that for any  $h > 0$  and any  $n \leq N_h$ ,  $|y_k^h| \leq R$ . Thus taking into account (3), there exists  $M_R$  such that

$$\forall h > 0, \forall k \leq N_h, \forall u \in U, |f(y_k^h, \alpha_k, u)| \leq M_R.$$

The proof of Theorem 2 is carried out in three steps.

### Step 1

Let us show that there exists  $\kappa > 0$  such that:

$$V_Q(y_0^h) \geq V_Q(y_0^h + hf^h(y_0^h, \alpha_0, u_0^h))e^{-\lambda h} + \lambda hg_Q(y_0^h) - \kappa h^2 - 2E_h. \quad (12)$$

For simplicity, we will note here  $y_0^h = y_0$ , and  $u_0^h = u_0$ . Recall that the dynamical programming principle for  $V_Q$  writes as:

$$V_Q(y_0) = \min_{u \in Y} \max_{\alpha \in \mathcal{A}} \left[ V_Q(y_{y_0}^{\alpha, u[\alpha]}(h))e^{-\lambda h} + \int_0^h g_Q(y_{y_0}^{\alpha, u[\alpha]}(t))e^{-\lambda t} dt \right]. \quad (13)$$

Let  $\bar{u}_0 \in Y$  be the minimizing strategy for this problem. Let  $\alpha^*$  be an approximation of the uncertainties, satisfying  $\alpha^*(t) = \alpha_k$  for any  $t \in [kh, (k+1)h)$ . Then the following inequality holds:

$$V_Q(y_0) \geq V_Q(y_{y_0}^{\alpha^*, \bar{u}_0[\alpha^*]}(h))e^{-\lambda h} + \int_0^h g_Q(y_{y_0}^{\alpha^*, \bar{u}_0[\alpha^*]}(t))e^{-\lambda t} dt. \quad (14)$$

We denote  $\bar{u}_0[\alpha^*] = \mathbf{u}_0 \in \mathcal{U}$ .

Let us consider the first term of the right-hand member of inequation (14). By convexity of  $f(x, \alpha, \mathcal{U})$  for any  $x \in \mathbb{R}^n$  and  $\alpha \in A$ , there exists  $u_0^* \in U$  such that

$$y_0 + \int_0^h f(y_0, \alpha_0, \mathbf{u}_0(t)) dt = y_0 + hf(y_0, \alpha_0, u_0^*).$$

Then,  $y_{y_0}^{\alpha^*, \mathbf{u}_0}$  the trajectory starting at  $y_0$  for  $t = 0$  and following uncertainties  $\alpha^*$  and control  $\mathbf{u}_0$  satisfies  $|y_{y_0}^{\alpha^*, \mathbf{u}_0}(h) - y_0| \leq M_R h$ . Moreover:

$$\begin{aligned} |y_{y_0}^{\alpha_0, \mathbf{u}_0}(h) - y_0 - hf(y_0, \alpha_0, u_0^*)| &\leq \int_0^h |f(y_{y_0}^{\alpha_0, \mathbf{u}_0}(t), \alpha_0, \mathbf{u}_0(t)) - f(y_0, \alpha_0, \mathbf{u}_0(t))| dt \\ &\leq \int_0^h M_0 |y_{y_0}^{\alpha_0, \mathbf{u}_0}(t) - y_0| dt \leq M_0 M_R h^2, \end{aligned}$$

where  $M_0$  is the Lipschitz coefficient of  $f$ .

Moreover, using  $f^h$  the approximation of  $f$ :

$$|y_{y_0}^{\alpha_0, \mathbf{u}_0}(h) - y_0 - hf^h(y_0, \alpha_0, u_0^*)| \leq M_0 M_R h^2 + \kappa_R h^2.$$

From 2 we know that  $V_Q$  is a Lipschitz continuous function on  $\mathbb{R}^2$ ; thus by denoting  $L_V$  its Lipschitz coefficient:

$$|V_Q(y_{y_0}^{\alpha_0, \mathbf{u}_0}(h)) - V_Q(y_0 + hf^h(y_0, \alpha_0, u_0^*))| \leq L_V |y_{y_0}^{\alpha_0, \mathbf{u}_0}(h) - y_0 - hf^h(y_0, \alpha_0, u_0^*)|,$$

which leads to:

$$\begin{aligned}
V_Q(y_{y_0}^{\alpha_0, \mathbf{u}_0}(h)) &\geq V_Q(y_0 + hf^h(y_0, \alpha_0, u_0^*)) - L_V(M_0 M_R + \kappa_R)h^2, \\
&\geq V_Q^h(y_0 + hf^h(y_0, \alpha_0, u_0^*)) - L_V((M_0 M_R + \kappa_R)h^2 - E_h), \\
&\geq V_Q^h(y_0 + hf^h(y_0, \alpha_0, u_0)) - L_V((M_0 M_R + \kappa_R)h^2 - E_h), \quad (\text{by definition of } u_0) \\
&\geq V_Q(y_0 + hf^h(y_0, \alpha_0, C_0)) - L_V((M_0 M_R + \kappa_R)h^2 - 2E_h).
\end{aligned}$$

We now deal with the second term of (14). Since the function  $g_Q$  is 1-Lipschitz, we get that for any  $t \in [0, h]$ :

$$|g_Q(y_{y_0}^{\alpha^*, \mathbf{u}_0}(t)) - g_Q(y_0)| \leq \int_0^t |f(y_{y_0}^{\alpha_0, \mathbf{u}_0}(s), \alpha_0, \mathbf{u}_0(s))| ds \leq \kappa_R t,$$

which leads to:

$$\int_0^h g_Q(y_{y_0}^{\alpha^*, \mathbf{u}_0}(t))e^{-\lambda t} dt \geq \int_0^h g_Q(y_0)e^{-\lambda t} dt - \int_0^h \kappa_R t e^{-\lambda t} dt \geq \lambda h g_Q(y_0) - \kappa_R \frac{h^2}{2}.$$

Going back to (14), we get that:

$$V_Q(y_0) \geq V_Q(y_0 + hf^h(y_0, \alpha_0, u_0))e^{-\lambda h} - L_V(LM_R + \kappa_R)h^2 - 2E_h + \lambda h g_Q(y_0) - L_g \kappa_R \frac{h^2}{2}$$

which concludes the demonstration of (12) by setting  $\kappa = L_V(LM_R + \kappa_R) + L_g \kappa_R/2$ .

## Step 2

We can generalize (12) to any  $k < N_h$ :

$$V_Q(y_k) \geq V_Q(y_k + hf^h(y_k, \alpha_k, u_k))e^{-\lambda h} + \lambda h g_Q(y_k) - 2E_h - \kappa h^2.$$

Moreover,

$$\begin{aligned}
V_Q(y_0) &\geq V_Q(y_1)e^{-\lambda h} + \lambda h g_Q(y_0) - 2E_h - \kappa h^2 \\
&\geq V_Q(y_2)e^{-2\lambda h} + \lambda h(g_Q(y_0) + e^{-\lambda h} g_Q(y_1)) - 4E_h - 2\kappa h^2.
\end{aligned}$$

By induction we deduce that:

$$V_Q(y_0) \geq V_Q(y_{N_h})e^{-\lambda N_h h} + \lambda h \sum_{k=0}^{N_h-1} e^{-\lambda k h} g_Q(y_k) - 2N_h E_h - \kappa N_h h^2$$

## Step 3

Now consider the complete integral  $\int_0^{T_h} e^{-\lambda t} g_Q(\mathbf{y}^h(t)) dt$ . We have that:

$$\begin{aligned}
\int_0^{T_h} e^{-\lambda t} g_Q(\mathbf{y}^h(t)) dt &= \sum_{k=0}^{N_h-1} \int_{kh}^{(k+1)h} e^{-\lambda t} g_Q(\mathbf{y}^h(t)) dt = \sum_{k=0}^{N_h-1} e^{-\lambda kh} \int_0^h e^{-\lambda t} g_Q(\mathbf{y}^h(t + kh)) dt \\
&\leq \sum_{k=0}^{N_h-1} e^{-\lambda kh} \int_0^h (g_Q(y_k) + t C_R) dt \leq \sum_{k=0}^{N_h-1} e^{-\lambda kh} \left( \lambda h g_Q(y_k) + \frac{h^2}{2} C_R \right).
\end{aligned}$$

Moreover,

$$\int_{T_h}^{+\infty} e^{-\lambda t} g_Q(\mathbf{y}^h(t)) dt \leq \|g_Q\|_{\infty} e^{-\lambda T_h}.$$

Thus,

$$V_Q(y_0) \geq \int_0^{+\infty} e^{-\lambda t} g_Q(\mathbf{y}^h(t)) dt - h^2 N_h \left( \frac{C_R}{2} + \kappa \right) - 2N_h E_h - \|g_Q\|_{\infty} e^{-\lambda N_h h}. \quad (15)$$

This concludes the proof of (11), since using the assumptions (10), we get;

$$V_Q(y_0) \geq \limsup_{h \rightarrow 0} \int_0^{+\infty} e^{-\lambda t} g_Q(\mathbf{y}^h(t)) dt. \quad (16)$$

Finally, the functions  $(\mathbf{y}^h)$  are equicontinuous in  $W^{1,1}([0, +\infty), e^{-M_0 t})$ , so they have an accumulation point  $\mathbf{y} \in W^{1,1}([0, +\infty), e^{-M_0 t})$ . Using (16), we have:

$$0 = V_Q(y_0) \geq \int_0^{+\infty} e^{-\lambda t} g_Q(\mathbf{y}(t)) dt.$$

Therefore, the trajectory is viable, which concludes the proof of Theorem 2. □

*Remark 4.* It is possible that, for a fixed  $h > 0$ , the constructed trajectory  $\mathbf{y}^h$  is not viable on  $[0, T_h]$ . However, because of (16), for  $h$  small enough the trajectory stays close to  $\mathcal{N}_{\mathbb{T}_Q}$ .

Moreover, it is possible that for an initial point  $y_0$  that satisfies  $g_Q(y_0) = 0$  but  $V_Q(y_0) > 0$ , for certain realizations of the uncertainties  $\bar{\alpha}$ , the trajectory  $\mathbf{y}$  constructed by Algorithm 1 is viable.

In Algorithm 1, the uncertainty function  $\bar{\alpha}$  is supposed to be known. This is obviously the case when the problem is without uncertainty. This algorithm is also of interest when the model is with uncertainties. It provides a tool to explore different scenarios and adjust the control depending on the variations of these uncertainties.

It is also possible to modify the algorithm to define the worst case scenario and to compute the best response to that scenario. In this case, the algorithm should be modified as shown in Algorithm 2.

---

#### Algorithm 2 Stability (worst case)

---

The starting point  $y$  is known.

*Initialization* Set  $y_0^h = y$ .

*Recursive definition of  $y_k^h$*  Suppose  $(y_\ell^h)$  is known for  $\ell = 0 \dots k-1$ . To determine  $y_k^h$ , we first define the worst value of uncertainties:

$$\alpha_k^h \in \operatorname{argmax}_{\alpha \in A} \min_{u \in U} V_Q^h(y_{k-1}^h + h f^h(y_{k-1}^h, \alpha, u)) e^{-\lambda h} + \lambda h g_Q(y_{k-1}^h).$$

Then we consider the optimal control  $u_k^h$  such that:

$$u_k^h \in \operatorname{argmin}_{u \in U} V_Q^h(y_{k-1}^h + h f^h(y_{k-1}^h, \alpha_k^h, u)) e^{-\lambda h} + \lambda h g_Q(y_{k-1}^h).$$

The new position is then defined by:

$$y_k^h = y_{k-1}^h + h f^h(y_{k-1}^h, \alpha_k^h, u_k^h).$$

*Complete trajectory* We associate to the sequence of controls  $(u_k^h)_k$  the piecewise constant function  $\mathbf{u}^h(t) = u_k^h$  for  $t \in [kh, (k+1)h)$ , and an approximate trajectory  $\mathbf{y}^h$  defined on  $[0, +\infty)$  by:

$$\begin{cases} \dot{\mathbf{y}}^h(t) = f^h(y_k^h, \alpha_k^h, u_k^h) & \text{for } t \in (kh, (k+1)h) \\ \mathbf{y}^h(kh) = y_k^h & \forall k \in \mathbb{N}, k \leq N_h \\ \dot{\mathbf{y}}^h(t) = f(\mathbf{y}(t), \bar{\alpha}, 0) & \forall t > T_h \end{cases}$$


---

*Remark 5.* Algorithm 2 provides a robust trajectory with respect to any uncertainty within the range of interval  $A$ . This trajectory can be seen as a trajectory of total "victory", but it can also be seen as a pessimistic trajectory because it is foreseen in the worst case. In this perspective, the trajectories of Algorithm 1 are less pessimistic because they adjust to the value of the uncertainty if it becomes available (by measurement for example) as the trajectory evolves.

## 4.2 | Minimal entry time

We now study how to construct optimal trajectories, knowing an approximation of  $W$ , entering  $\mathcal{N}_{\mathbb{T}_Q}$  in a minimal time. We focus on system (M1), an extension to (M2) can be obtained with results from<sup>15</sup>.

The first algorithm we present is a direct application of the value function  $W$ . Suppose an approximation  $W^h$  of  $W$  has been constructed. Choose a starting point  $x_0$  such that  $W^h(x_0, T) < 0$ . Given a fixed perturbation  $\bar{\alpha} \in \mathcal{A}$ , and maximal number of time steps  $N$  (the fixed time step being  $h = T/N$ ), we define the trajectory reconstruction by Algorithm 3

---

### Algorithm 3 Minimal entry time

---

The starting point  $x_0$  and the uncertainties realization  $\bar{\alpha} := (\bar{\alpha}_k)_k$  are known.

*Initialization* Set  $y_0^h = x_0$ .

*Recursive definition of  $y_\ell^h$*  Suppose  $(y_\ell^h)$  is known for  $\ell = 0 \dots k-1 < N$ . To determine  $y_k^h$ , we define an optimal control  $u_k^h$  such that:

$$u_k^h \in \operatorname{argmin}_{u \in U} W^h(y_{k-1}^h + hf^h(y_{k-1}^h, \bar{\alpha}_k, u), kh)$$

The new position is then defined by:

$$y_k^h = y_{k-1}^h + hf^h(y_{k-1}^h, \alpha_k, u_k^h).$$

*Complete trajectory* We associate to the sequence of controls  $(u_k^h)_{0 \leq k \leq N-1}$  the piecewise constant function  $\mathbf{u}^h(t) = u_k^h$  for  $t \in ]kh, (k+1)h]$ , and an approximate trajectory  $\mathbf{y}^h$  defined on  $[0, T]$  by:

$$\begin{cases} \mathbf{y}^h(kh) = y_k^h & \forall n \in \mathbb{N}, n \leq N \\ \dot{\mathbf{y}}^h(t) = f^h(y_k^h, \alpha_k, u_k^h) & \text{for } t \in (kh, (k+1)h], k < N. \end{cases}$$


---

We suppose that there exists  $E_h > 0$  such that  $E_h/h \rightarrow 0$  when  $h \rightarrow 0$  and:

$$\forall t > 0, \|W(\cdot, t) - W^h(\cdot, t)\|_\infty \leq E_h.$$

Then the following convergence theorem holds:

**Theorem 3.** Let  $y \in \mathbb{R}^2$  and let  $(y_k^h)$  be the sequence defined by Algorithm 3. We suppose true the assumptions  $(\mathbf{H}_f)$  and  $(\mathbf{H}_{A1})$ - $(\mathbf{H}_{A2})$ . Then the functions  $(\mathbf{y}^h)$  form a better than minimizing sequence in the following sense:

$$\forall t \in [0, T], W(x, t) \leq \limsup_{h \rightarrow 0} d_Q(\mathbf{y}^h(t))$$

Moreover, the family of functions  $\mathbf{y}^h$  admits cluster points as  $h \rightarrow 0$ . Any such cluster  $\bar{\mathbf{y}}$  is a trajectory of system (M1) with uncertainties  $\alpha$ .

This theorem can be proven by using similar arguments as in the proof of theorem (11).

*Remark 6.* As there might be several controls such that the trajectory is optimal, the control found by Algorithm 3 might present lots of variations depending on the implementation of the argmin function. Moreover, recall that  $u$  represents a dosage of drug to give to a patient (or to put on a Petri dish as a first biological model). Thus, shattering controls are really not interesting for a medical application. Gratefully, as shown in Section 5, the controls found numerically are rarely shattering, so their actual implementation would be feasible.

In Algorithm 3, the the realization of the uncertainties is supposed to be known. To have a better hindsight of the adaptability of the system, we can consider the worst case scenario, were the uncertainties always take the worst value possible to delay the entrance in  $\mathcal{N}_{\mathbb{T}_Q}$ . In this case, the corresponding trajectories can be obtained by Algorithm 4.

*Remark 7.* As mentioned in Remark 5, the worst case (Algorithm 4) provides an admissible trajectory that can reach the stability kernel for any uncertainty within the set  $A$ , whereas Algorithm 3 provides a less pessimistic trajectory that can reach a target and adjust to the values of the uncertainties if they become available.

**Algorithm 4** Minimal entry time (worst case)

The starting point  $x_0$  is known.

*Initialization* Set  $y_0^h = x_0$ .

*Recursive definition of  $y_\ell^h$*  Suppose  $(y_\ell^h)$  is known for  $\ell = 0 \dots k-1 < N$ . To determine  $y_k^h$ , we first define the worst value of the uncertainties:

$$\alpha_k^h \in \operatorname{argmax}_{\alpha \in A} \min_{u \in U} W^h(y_{k-1}^h + hf^h(y_{k-1}^h, \bar{\alpha}_k, u), kh)$$

We then consider the optimal control  $u_k^h$  such that:

$$u_k^h \in \operatorname{argmin}_{u \in U} W^h(y_{k-1}^h + hf^h(y_{k-1}^h, \bar{\alpha}_k^h, u), kh)$$

The new position is then defined by:

$$y_k^h = y_{k-1}^h + hf^h(y_{k-1}^h, \alpha_k^h, u_k^h).$$

*Complete trajectory* We associate to the sequence of controls  $(u_k^h)_{0 \leq k \leq N-1}$  the piecewise constant function  $\mathbf{u}^h(t) = u_k^h$  for  $t \in ]kh, (k+1)h]$ , and an approximate trajectory  $\mathbf{y}^h$  defined on  $[0, T]$  by:

$$\begin{cases} \mathbf{y}^h(kh) = y_k^h & \forall n \in \mathbb{N}, n \leq N \\ \dot{\mathbf{y}}^h(t) = f^h(y_k^h, \alpha_k^h, u_k^h) & \text{for } t \in (kh, (k+1)h], k < N. \end{cases}$$

**5 | NUMERICAL SIMULATIONS**

We present in this section numerical simulations solving the viability and reachability problems. The simulations were performed with the software ROC-HJ. The values of the different parameters are listed in table 1. These parameters were chosen arbitrarily to show some general numerical results.

Parameter	Symbol	Value for numerical simulations
Growth rate	$\rho$	1.0
Capacity	$K$	3.0
Metabolism difference	$m$	2.0
Size threshold	$Q$	1.3 (Q=0.8 in Test 1)
Maximal time of treatment	$T$	2, 5 or 10
Global health indicator renewal	$\rho_w$	1.0
Global health indicator evacuation	$\mu$	1
Drug effect on the global health	$\nu$	1.0
Drug threshold for the global health	$u_{\text{tox}}$	6.0
Maximal drug dosage	$U_{\text{max}}$	10.0
Minimal/Maximal drug efficiency	$\gamma_{\text{min}}, \gamma_{\text{max}}$	$0.1 \pm \delta$
Minimal/Maximal competition force	$\beta_{\text{min}}, \beta_{\text{max}}$	$2/3 \pm \delta$
Range of uncertainties	$\delta$	0.0% (Tests without uncertainties), 2.0%, 5.0%, 7.5%, or 10.0%

**TABLE 1** List of parameters and their values for numerical simulations

To solve the viability and reachability problems formulated in the previous sections, we proceed by solving the corresponding Hamilton Jacobi equations. We first start with some simulations for model (M1) when there is no uncertainties in the model, in other words when the set  $\mathcal{A}$  is reduced to a singleton.

## 5.1 | Numerical approximation of the value functions $V_Q$ and $W$

Following Theorem 1, we know that the value function  $V_Q$ , corresponding to the viability problem, is the unique solution of a steady HJ equation in the following form:

$$\lambda V_Q + H(x, \nabla V_Q) - g_Q(x) = 0, \quad x \in \mathbb{R}^n,$$

where  $\lambda > M_0$  and the Hamiltonian  $H$  is defined in Theorem 1. An approximation of  $V_Q$  can be obtained by a numerical discretization of this HJ equation. Note that numerical approximations of HJ equations have been studied extensively in the literature. One can cite for instance the Semi-Lagrangian methods<sup>28,29,30</sup>, or the class of finite differences methods. It is known that a Semi-Lagrangian scheme would require a discretization of the set of the control variables. Since we have an explicit formula of  $H$ , we prefer to use a scheme that will exploit this structure of the Hamiltonian and hence avoid the discretization of the control variables. For this reason, in all our simulations we will use a scheme based on finite difference approximations. Let  $\Delta y = (\Delta y_k)_{1 \leq k \leq n}$  be a spatial discretization step (with  $\Delta y_k > 0$ ). Consider a uniform grid on  $\mathbb{R}^n$  as follows:

$$\mathcal{G} := \{y_i = i\Delta y \equiv (i_k \Delta y_k)_{1 \leq k \leq n}, i = (i_1, \dots, i_n) \in \mathbb{Z}^n\}. \quad (17)$$

Denote  $\{e_k\}_{k=1, \dots, n}$  the canonical basis of  $\mathbb{R}^n$ . For a function  $V : \mathcal{G} \rightarrow \mathbb{R}$ , the terms  $D_k^\pm V(x)$  are given by:

$$D_k^\pm V(x) := \pm \frac{V(x \pm \Delta y_k e_k) - V(x)}{\Delta y_k}. \quad (18)$$

The vectors  $D^\pm V(x)$  are defined by:  $D^\pm V(x) := (D_1^\pm V(x), \dots, D_n^\pm V(x))$ . An approximation of  $V_Q$  can be obtained by solving the following approximated scheme:

$$V^h(x) = (1 - \lambda h)V^h(x) - H^\Delta(x, D^+ V^h(x), D^- V^h(x)) + g(x) \quad \text{for } x \in \mathcal{G}, \quad (19)$$

where the numerical Hamiltonian  $H^\Delta$  is an approximation of the Hamiltonian function  $H$ . The numerical approximation  $V^h : \mathbb{R}^n \rightarrow \mathbb{R}$  is a bilinear interpolation of  $\{V^h(x), x \in \mathcal{G}\}$ .

Following<sup>31,15</sup>, if the numerical Hamiltonian  $H^\Delta$  is Lipschitz continuous on all its arguments, consistent with  $H$  (i.e.,  $H^\Delta(y, p, p) = H(y, p)$ ) and monotone (i.e.  $\frac{\partial H^\Delta}{\partial p_k^-}(y, p^-, p^+) \geq 0$ ,  $\frac{\partial H^\Delta}{\partial p_k^+}(y, p^-, p^+) \leq 0$ ) together with the following Courant-Friedrich-Levy (CFL) condition

$$h \sum_{k=1}^n \frac{1}{\Delta y_k} \left\{ \left| \frac{\partial H^\Delta}{\partial p_k^-}(y, p^-, p^+) \right| + \left| \frac{\partial H^\Delta}{\partial p_k^+}(y, p^-, p^+) \right| \right\} \leq 1,$$

then, as  $h$  goes to 0, the numerical solution  $V^h$  converges uniformly, on every compact set, towards the desired solution  $V_Q$ .

In this paper, a simple Lax-Friedrich scheme has been used:

$$H^\Delta(x, p^-, p^+) := H(y, \frac{p^- + p^+}{2}) - \sum_{k=1}^n \frac{c_k}{2} (p_k^+ - p_k^-),$$

with constants  $c_k \geq |\frac{\partial H}{\partial p_k}|$ , and a fictitious time step  $h$  such that:

$$h \sum_{k=1}^n \frac{c_k}{\Delta y_k} \leq 1. \quad (20)$$

Although (19) is a nonlinear equation, the use of a fictitious time  $h$  such that  $h\lambda < 1$  guarantees that the following fixed-point algorithm converges towards a unique solution that happens to be  $V^h$  (see<sup>23,28,30</sup>):

- For  $k = 0$ , consider  $V^{h,0}$  a given function on the domain of computation  $\mathcal{D}$
- For  $k \geq 0$ , compute  $V^{h,k+1}$  by:

$$V^{h,k+1}(x) = (1 - \lambda h)V^{h,k} - H^\Delta(x, D^+ V^{h,k}(x), D^- V^{h,k}(x)) + g(x) \quad \text{for } x \in \mathcal{G}. \quad (21)$$

In practice, the above fixed-point algorithm stops at a stopping criteria:

$$\|V^{h,k+1} - V^{h,k}\|_\infty \leq \varepsilon,$$

where  $\varepsilon$  is a given tolerance. In all our simulations, this tolerance will be set to  $\varepsilon = 1e - 8$ .



*Remark 8.* Instead of a fixed-point algorithm described here above, one can use a policy iterations method (or Howard algorithm), see<sup>32,33</sup>. In the rest of the paper, we prefer to focus on the analysis of the obtained results and not on the performances of the numerical schemes. We simply use the Lax-Friedrich scheme coupled with a fixed-point algorithm.

An approximation of  $W$  is now determined through the following scheme. Let  $N$  a given integer, denote  $\Delta t$  the time discretization step such that  $T/N = dt$ . Set  $t_\ell := \ell \Delta t$ , and denote by  $w_i^\ell$  an approximation of the solution  $W(t_\ell, y_i)$ . By using again the Lax-Friedrich scheme, we consider the explicit scheme, as in<sup>15</sup>:

$$w_i^\ell = \max \left( w_i^{\ell+1} - \Delta t H^\Delta (y_i, D^- w_i^{\ell+1}, D^+ w_i^{\ell+1}), w_i^\ell - g_w(y_i) \right), \quad (22a)$$

$$\ell \in \{1 \dots, N\} \quad y_i \in \mathcal{G}$$

$$w_i^0 = V_Q(y_i) \quad \text{for } y_i \in \mathcal{G}, \quad (22b)$$

and we denote  $W^\Delta$  the interpolation of  $(W_i^\ell)_{l,i}$  on  $(t_l, x_i)_{l,i}$ .

*Remark 9.* Under the CFL condition:

$$\Delta t \sum_{k=1}^n \frac{c_k}{\Delta y_k} \leq 1,$$

the scheme (22) produces a numerical approximation  $W^\Delta$  that converges to the desired solution  $W$ , as  $\Delta = (\Delta t, \Delta y)$  go to 0 (see<sup>15</sup> for more details).

Notice that Algorithm 2 of trajectory reconstruction requires the values of the approximate function  $W^\Delta$  at every time step  $t_\ell$ . It means, that the values  $w_i^\ell$  should be stored on the grid  $\mathcal{G}$  at each time step. To reduce the storage effort, we can use the **minimal** time function mapping  $\mathcal{T}$  defined in (8). Indeed, while computing the approximation  $W^\Delta$ , we can obtain and store an approximation  $\mathcal{T}^\Delta$  as follows:

For  $\ell = 0$ , set  $\mathcal{T}^{\Delta,0}(y_i) = 0$  if  $V_Q(y_i) \leq 0$ , and  $\mathcal{T}^{\Delta,0}(y_i) = +\infty$  otherwise;

For  $\ell \geq 1$ , once  $w_i^\ell$  is computed, the minimum time function can be updated by:

$$\mathcal{T}^{\Delta,\ell}(y_i) = \begin{cases} t_\ell & \text{if } w_i^\ell \leq 0 \text{ and } \mathcal{T}^{\Delta,\ell-1}(y_i) = +\infty, \\ \mathcal{T}^{\Delta,\ell-1}(y_i) & \text{otherwise.} \end{cases}$$

An algorithm of reconstruction, based on the minimum time function  $\mathcal{T}^\Delta$  can be considered (instead of Algorithm 3). We describe it in Algorithm 5

---

#### **Algorithm 5** Minimal entry time, using $\mathcal{T}^\Delta$

---

Let  $x_0 \in \mathcal{K}$  be the starting point and consider the given uncertainty realization  $\bar{\alpha}$ .

*Initialization* Set  $y_0^h = x_0$ .

*Recursive definition of  $y_\ell^h$*  Suppose  $(y_\ell^h)$  is known for  $\ell = 0 \dots k-1 < N$ . To determine  $y_k^h$ , we define an optimal control  $u_k^h$  such that:

$$u_k^h \in \operatorname{argmin}_{u \in U} \mathcal{T}^h(y_{k-1}^h) + h f^h(y_{k-1}^h, \bar{\alpha}_k, u)$$

The new position is then defined by:

$$y_k^h = y_{k-1}^h + h f^h(y_{k-1}^h, \bar{\alpha}_k, u_k^h).$$

*Complete trajectory* We associate to the sequence of controls  $(u_k^h)_{0 \leq k \leq N-1}$  the piecewise constant function  $\mathbf{u}^h(t) = u_k^h$  for  $t \in ]kh, (k+1)h]$ , and an approximate trajectory  $\mathbf{y}^h$  defined on  $[0, T]$  by:

$$\begin{cases} \mathbf{y}^h(kh) = y_k^h & \forall k \in \mathbb{N}, k \leq N \\ \dot{\mathbf{y}}^h(t) = f^h(y_k^h, \bar{\alpha}_k, u_k^h) & \text{for } t \in (kh, (k+1)h], k < N. \end{cases}$$


---

In general, the function  $\mathcal{T}$  is not Lipschitz continuous and there is no proof of convergence for Algorithm 5. However, in the simulations that we have performed in this section, we have considered both Algorithms 3 and 5, and the resulting trajectories are very similar. Algorithm 5 can thus be seen as a numerical tool to reduce the memory storage. For more details, we refer to<sup>34</sup>.

Next, we will present different simulations and discuss the results on the two models (M1) and (M2). Table 2 gathers all the parameters used in our simulations.

Domain of computation for model (M1)	$\mathcal{D} := [-0.1, 3.1] \times [-0.1, 1.6]$
# grid points	$320 \times 170$
Domain of computation for model (M2)	$\mathcal{D} := [-0.1, 3.1] \times [-0.1, 1.6] \times [0, 1.2]$
# grid points	$320 \times 170 \times 120$
Fictitious time $h$ in (19)	$2.6e-4$
Time step in (22)	$2.6e-4$
Stopping threshold $\varepsilon$ in (21)	$\varepsilon := 1e-8$

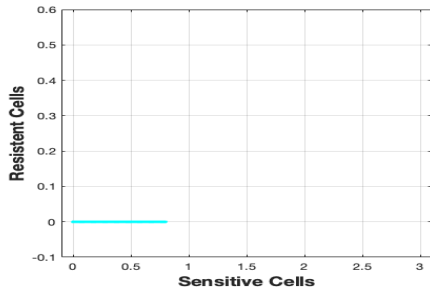
**TABLE 2** Parameters used in numerical reconstructions of functions  $V$  and  $W$ .

## 5.2 | Model without toxicity and without uncertainties

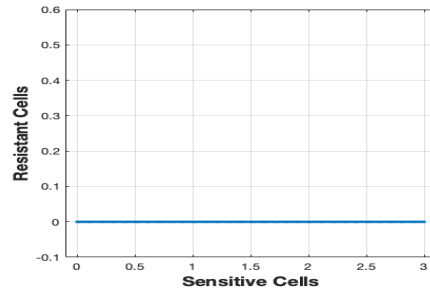
### Test 1

As stated in proposition 1, if  $Q < \frac{K}{1+K\beta_{\min}/\rho}$ , then the set  $\mathcal{N}_{\mathbb{T}_Q}$  is reduced to the segment  $\{(s, 0), s \in [0, Q]\}$ .

Our numerical resolution is robust enough to retrieve this result, as shown on Figure 2a. Furthermore, for  $T$  large enough, one can check that the set of initial tumours that can be brought to  $\mathcal{N}_{\mathbb{T}_Q}$  is then reduced to  $\{(s, 0), s \in [0, K]\}$ , which we can also numerically observe in Figure 2b, for  $T = 10$ . If we chose a size threshold too small, the only tumours that can satisfy the objectives are the ones without any resistant cells. We do not represent trajectories corresponding to this problem here, as they are all part of the  $\{(s, 0), s \in [0, K]\}$  segment. Of course, this case is trivial, and the aim of this simulation is just to show that the methodology works even when the capture basin has an empty interior.



(a) Stability set (in green)



(b) Reachability set (in blue) at  $T = 10$

**FIGURE 2** (Test 1) - Model (M1) with  $Q = 0.8$ .

### Test 2

In this test, we consider the model (M1) with  $Q = 1.3$ . We first compute the stability kernel  $\mathcal{N}_{\mathbb{T}_Q}$  which is displayed in Figure 3. In this figure, some viable trajectories and the corresponding control functions are represented.

More precisely, in Figure 3a, the computed stability kernel is represented as a filled zone and is limited by a dash line. Three viable trajectories are represented inside the stability kernel. On Figure 3b are displayed the control functions corresponding to the three trajectories. The time horizon chosen for this display is  $T = 20$ . In Figures 3c and 3d, we show the two components of the stable trajectories. In this figure and all the following, for every displayed trajectory, we use a different color and line style that is the same also used for the corresponding control function.

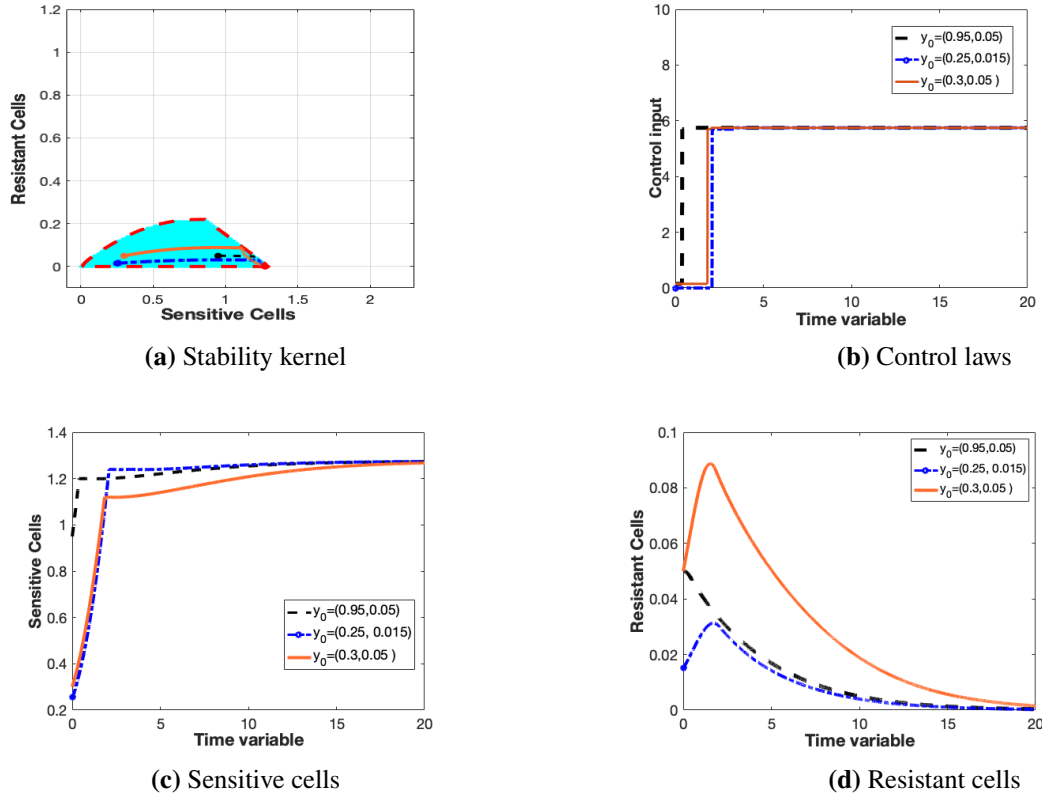


**FIGURE 3** (Test 2) - Model (M1) with  $Q = 0.13$ , stability kernel  $\mathcal{N}_{T_Q}^*$  and some viable trajectories

One can notice that the controls for each trajectory, after a certain amount of time without treatment, do not reach the maximal control value  $U_{\max}$ , but reach an intermediate value. Moreover, the trajectories seem to be attracted to a region on the  $\{(s, 0), s \in [0, Q]\}$  segment. As stated in Proposition 1, this segment contains points that are stable and locally attractive for certain constant values of the control  $u$ : the stability problem is thus numerically solved, here, by reaching their basin of attraction and setting the control value to the corresponding fixed control.

Moreover, in this case, setting the control law  $u(\cdot)$  to a high value near  $U_{\max}$ , even for a short time, could make the system escape  $\mathcal{N}_{T_Q}^*$ . Indeed, the trajectory under control  $U_{\max}$  starting from any point in  $\mathcal{N}_{T_Q}^*$  is rapidly shifted to the left (corresponding to a fast elimination of sensitive cells  $s$ ), thus if the treatment is not stopped early enough, the system would exit  $\mathcal{N}_{T_Q}^*$  by its left-side border.

### Test 3

Here, we still consider the case of Model (M1) with  $Q = 1.3$ . Now, we consider the reachability problem where we want to steer the trajectories to the stability kernel  $\mathcal{N}_{T_Q}^*$  computed in Test 2.

Figure 4 shows the capture basin  $\mathcal{R}(T)$  (filled, blue region) corresponding to the positions from where there exist trajectories that can reach the stability kernel  $\mathcal{N}_{T_Q}^*$  in a time less than  $T = 2$  (figure 4a) and in a time less than  $T = 10$  (figure 4b). In the same figures, some trajectories are represented. These trajectories correspond to the optimal paths starting from some initial positions outside the stability kernel and that reach the stability kernel in a minimum time less than  $T$ . The same trajectories along with the associated control functions are also displayed in Figure 5.

The trajectories shown here all exhibit the same behaviour: two phases of control can be observed, a first one with no treatment, and a second one with a maximal line of treatment, as pictured on Figure 5c. During the first phase, the sensitive cells population usually increases as seen on Figure 5a, while the resistant cells population globally decreases, as seen on Figure 5b. During the second phase, we see a decrease in the sensitive cells population, and a stabilization of the resistant cells population.

This can be expressed through the following biological interpretation. Since the control only acts on sensitive cells  $s$ , and that resistant cells are repressed only through competition with sensitive cells, a tumour can be treated only if sensitive cells already

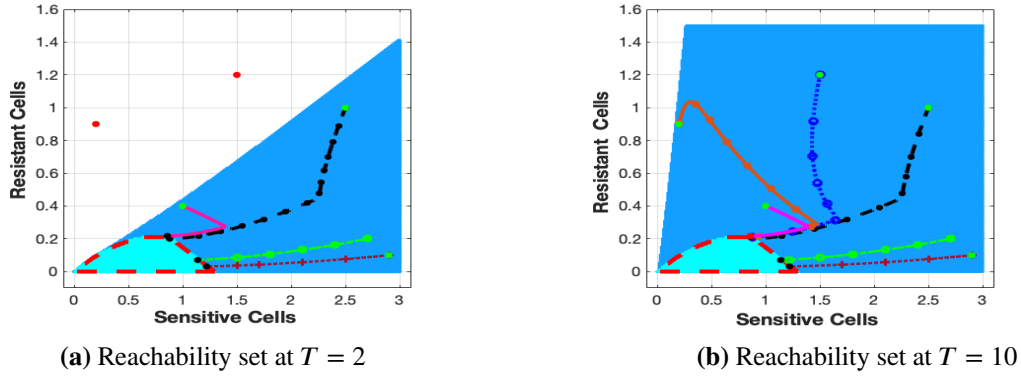


FIGURE 4 (Test 3) - Model (M1) with  $Q = 1.3$ , different capture basins

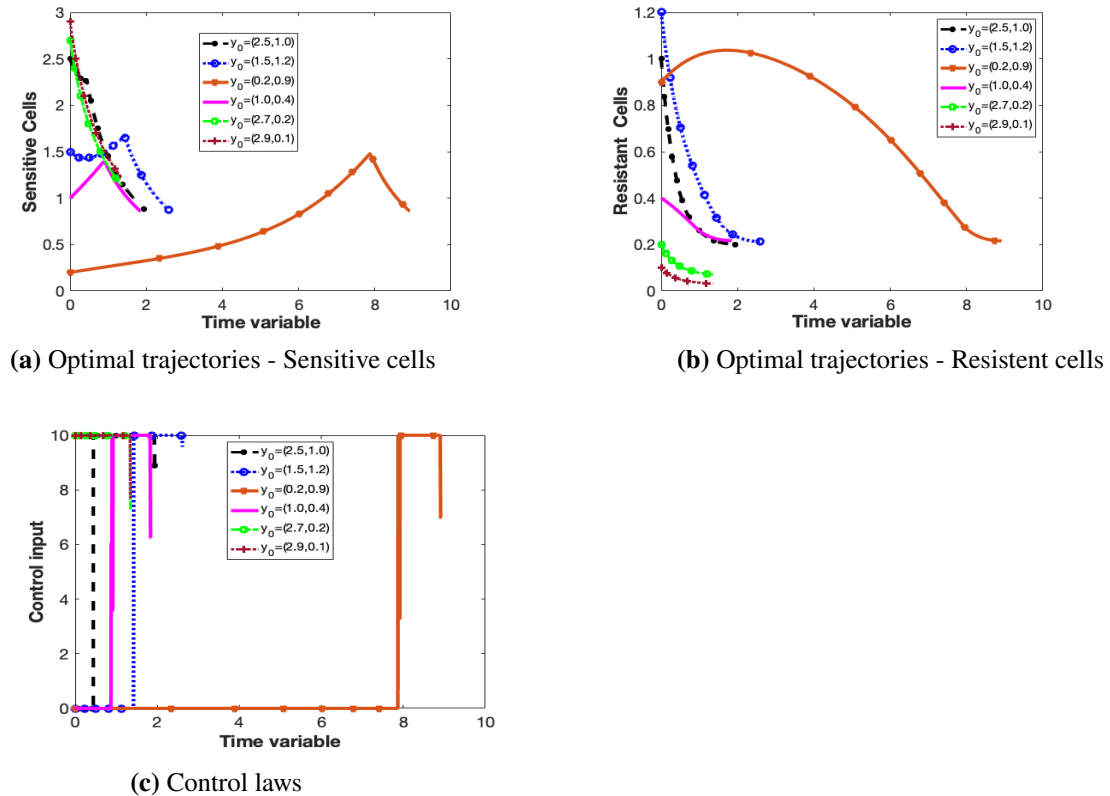


FIGURE 5 (Test 3) - Model (M1) with  $Q = 1.3$ . Some trajectories in  $\mathcal{R}(T)$ , for  $T = 10$ .

have a numerical advantage over resistant cells. Thus, if a tumour is initially too resistant, it is more interesting to wait for it to be "resensitized" than to treat it immediately. Then, once sensitive cells are sufficiently present, the control is set to its maximal value in order to minimize the time of entry into  $\hat{\mathcal{N}}_{T_0}$ . This maximal dose period would then correspond to the loading charge treatment used in classical chemotherapies.

Using maximal doses on actual patients can be very harmful for their sane cells, because of the general toxicity of the drugs used. This is why system (M2) takes into account the effect of high doses of treatment on a quantity representing the global health of the patient. We expect that this should change the behaviour of the system for the reachability problem, but not for the stability problem.

### 5.3 | Model with toxicity and without uncertainties

Here, we consider the model (M2). Likewise in the simulations performed with model (M1), we first compute the stability kernel and then we compute the set of positions from where it is possible to find admissible trajectories that can reach this stability kernel in a time less than  $T = 10$ .

The stability kernel  $\mathcal{N}_{\mathbb{T}_Q}$  is a 3-dimensional object, we represent a section of this kernel for a fixed value of the indicator  $w(0) = \frac{\rho_w}{\mu}$ . The trajectories represented on the phase planes are projections of the 3-dimensional trajectories on the 2-dimensional plane. For the reachability problem, we also represent only the section of  $\mathcal{R}(T)$  for  $w = \frac{\rho_w}{\mu}$ .

#### Test 4

Figure 6a displays the stability set  $\mathcal{N}_{\mathbb{T}_Q}$  for a fixed initial indicator  $w(0) = \frac{\rho_w}{\mu}$ . This corresponds to a patient initially healthy.

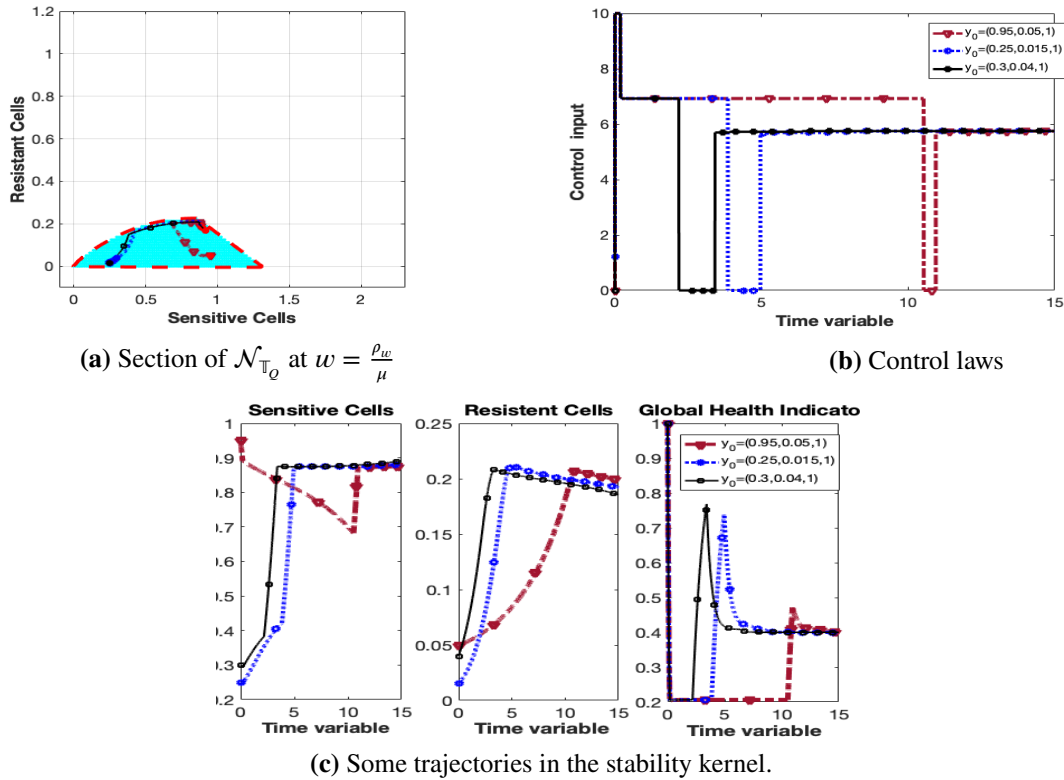


**FIGURE 6** (Test 4) - Model (M2): approximation of the stability kernel and some viable trajectories.

As expected, the stability kernel, displayed on Figure 6a, looks quite similar to the stability kernel for model (M1). This is because of our choice of parameters  $Q$  and  $u_{tox}$ .

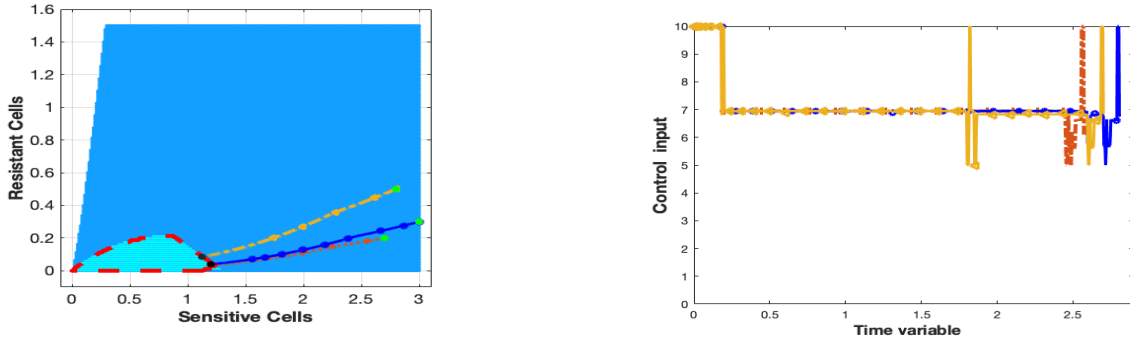
Indeed, we chose  $Q$  such that the control  $u \equiv u_Q = \frac{\rho}{\gamma} \left(1 - \frac{Q}{K}\right)$ , for which the point  $(Q, 0, w_0)$  is stable and attractive, is small enough so that  $w_0 = \frac{\rho_w}{\mu + v(u_Q - u_{tox})}$  is greater than  $w_{min}$ . Thus some values of  $u$  smaller than  $u_{tox}$ , which do not affect the evolution of  $w$ , can be sufficient to remain in  $\mathcal{N}_{\mathbb{T}_Q}$ .

However, models (M1) and (M2) do not produce the same trajectories nor the same control laws. Figure 6c shows three trajectories, starting from three different positions  $y_0$  in  $\mathcal{N}_{\mathbb{T}_Q}$  and that stay forever in the stability kernel. The corresponding control inputs are given in figure 6b. As can be noticed in this figure, the control laws present periods of drug holiday (periods without drug application), which correspond on figure 6c to an increase of the global health indicator. The controls are constant by parts, which is interesting for further medical applications.

## Test 5

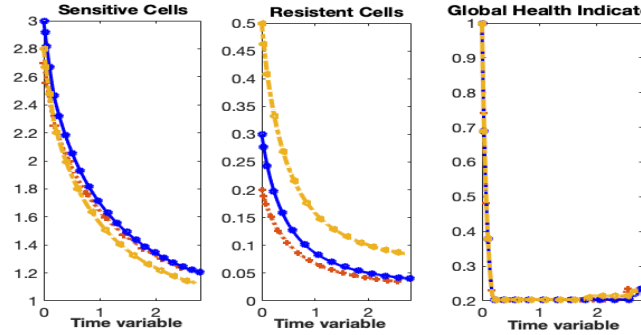
We now run simulations for the reachability problem for model (M2). We gather the resulting trajectories into three groups of similar structure.

Figure 7 presents a set of trajectories where the initial tumour is mostly sensitive to the treatment. The treatments begin with a maximal dosage, but since this is very toxic for the patient, the controls switch quickly to an intermediary value, as seen on Figure 7b. This intermediary value maintains the indicator  $w$  at its minimal value  $w_{\min}$ , as it can be seen on Figure 7c. This delays the time of entrance into  $\mathcal{N}_{T_0}$ , when compared to Figure 5 from model (M1).



(a) Capture set (section at  $w = \frac{\rho w}{\mu}$ ) at  $T = 10$ , and some projected optimal trajectories

(b) Control laws



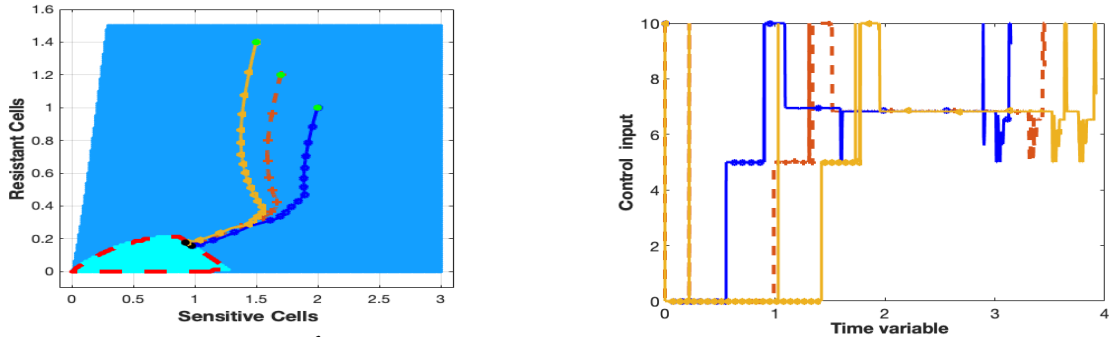
(c) Optimal trajectories (sensitive cells, resistant cells and global health indicator)

**FIGURE 7** (Test 5) - Reachability analysis for model (M2). Some trajectories corresponding to large sensitive initial tumours.

The set of trajectories gathered on Figure 8 represents tumours initially large and heterogeneous. As in model (M1), the control starts with an initial phase at  $u = 0$ , then switches to higher values, as pictured on figure 8b. Because of the toxicity constraint, except for short periods of time the control does not maintain  $u = U_{\max}$ . Instead, an intermediary value is selected, which maintains the indicator  $w$  at its minimal value, as pictured in Figure 8c.

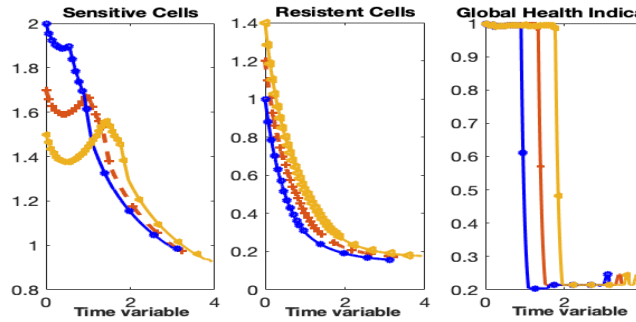
Finally, Figure 9 represents tumours that are initially very resistant to the chemotherapy. The controls gathered on figure 9b are very shattered, but present a global behaviour similar to previous results: a first phase without treatment to resensitize the tumour, then an increase in dose. The control finally mainly selects a value maintaining the indicator  $w$  at its minimal value.

We note that the model still favours the use of maximal treatment doses for the reachability problem, but for shorter periods of time, as it immediately increases the toxicity. Then, intermediary doses of treatment are preferred. During the intermediary doses arcs, we notice that the condition  $w(t) \geq w_{\min}$  is saturated: the global health indicator is at the lowest level the patient can endure.



(a) Capture basin (section at  $w = \frac{\rho_w}{\mu}$ ) at  $T = 10$  and some projected trajectories

(b) Control laws



(c) Trajectories: sensitive cells population, resistant cells population, global health indicator.

**FIGURE 8** (Test 5) - Reachability analysis for model (M2). A set of trajectories corresponding to large heterogeneous initial tumours.

#### 5.4 | Model with toxicity and with uncertainties

In this section, we consider again the model (M2), this time we assume that the treatment efficiency  $\gamma(\cdot)$  and the competition force  $\beta(\cdot)$  are unknown functions (i.e. there are uncertainties on some parameters of the model). In our simulations, we will consider the range of uncertainties for these functions are  $\pm 0\%$ ,  $\pm 5\%$ ,  $\pm 7.5\%$ , or  $\pm 10\%$ .

##### Test 6

Figure 10 presents sections of the stability kernel  $\mathcal{N}_{\mathbb{T}_0}$  and the reachability set  $\mathcal{R}(T)$  at time  $T = 5$ . In all these sections, the health indicator is fixed to the value  $w = \frac{\rho_w}{\mu}$ .

As it can be seen on Figure 10, as the range of uncertainties increases, the stable set  $\mathcal{N}_{\mathbb{T}_0}$  shrinks in size, and for a fixed time  $T$ , the reachability set  $\mathcal{R}(T)$  also appears smaller. Indeed, as the expected uncertainty on the parameters is bigger, the model is more pessimistic. Especially, with a range of uncertainties of  $\pm 10\%$ , both the sets are almost reduced to a segment, as seen on Figure 10d. With a medical application in mind, this tells us that if uncertainties on the parameters are too high, our method or the model might not be adapted to the objective.

Let us stress that the reachable sets represented in Figure 10 correspond to the set of initial positions from where it is always possible, for any uncertainty (within the prescribed range), to find a control strategy  $u(\cdot)$  such that the corresponding trajectory reaches the stability kernel and then stays there for ever.

Algorithm 4 provides robust trajectories corresponding to the worst case scenario. Figure 11 shows some of these robust trajectories, starting from different initial positions and that reach the stability kernel for any perturbation  $\alpha$  within a range of uncertainties of  $\delta = 7.5\%$ .

As mentioned in Remark 5, the robust trajectories might be too pessimistic. If the function  $\alpha$  becomes available, it is then possible to use Algorithm 5 to reconstruct an adjusted trajectory that takes into account the value of  $\alpha$ .

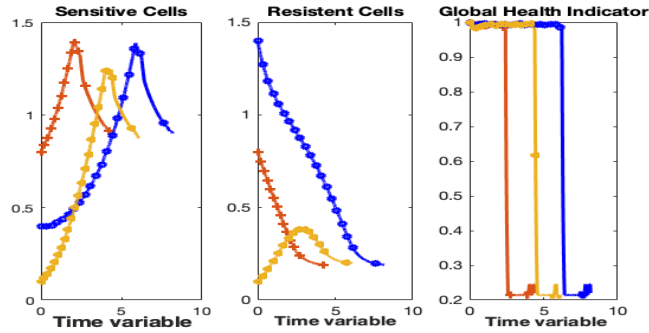
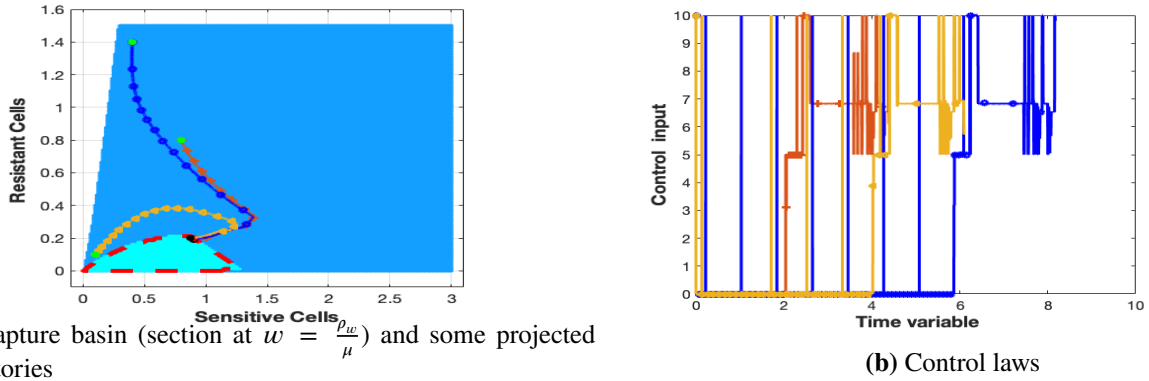


FIGURE 9 (Test 5) - Reachability analysis for model (M2). A set of trajectories corresponding almost resistant initial tumours.

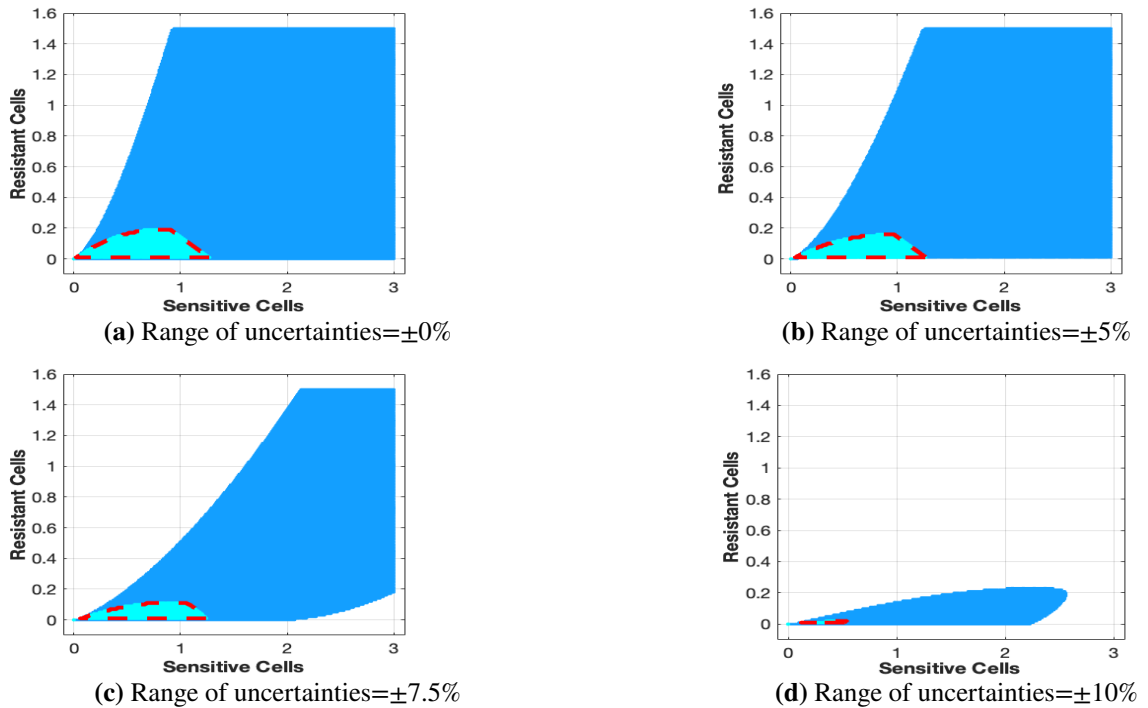


FIGURE 10 (Test 6) - Stability kernel (in cyan) and capture basin (in blue) at time  $T = 5$  for model (M2) with uncertainties



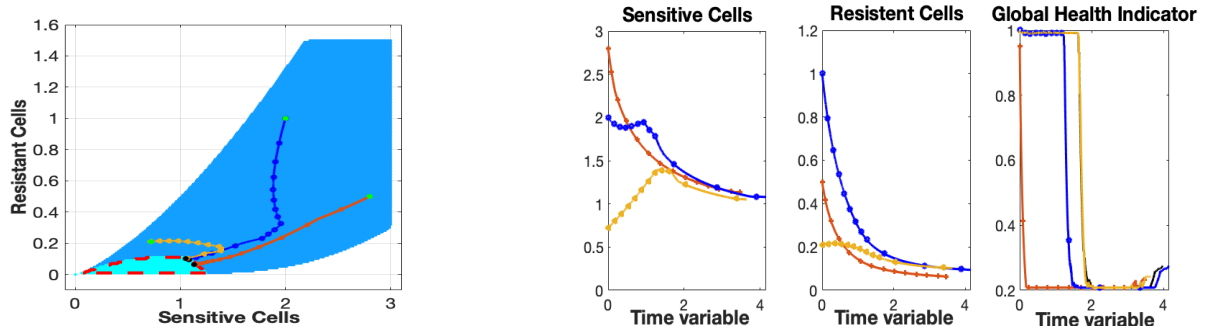


FIGURE 11 (Test 6) - Example of robust trajectories: range of uncertainties =  $\pm 7.5\%$

In Figure 12, we represent the trajectories, starting from the same initial position  $y_0 = (2.0, 1.0, 1.0)$ , and corresponding to four different functions  $\alpha_i := (\gamma_i, \beta_i)$  (for  $i = 1, \dots, 4$ ) within a range of uncertainties of  $\delta = 7.5\%$  (here,  $\bar{\gamma} = 0.1$ ,  $\bar{\beta} = 2/3$ ):

$$\gamma_1(t) = \begin{cases} \bar{\gamma}(1 + \delta) & \text{for } t \in [0, 1], \\ \bar{\gamma} & \text{for } t \in ]1, 2], \\ \bar{\gamma}(1 - \delta) & \text{for } t > 2, \end{cases} \quad \beta_1(t) = \begin{cases} \bar{\beta}(1 - \delta) & \text{for } t \in [0, 1], \\ \bar{\beta} & \text{for } t \in ]1, 2], \\ \bar{\beta}(1 + \delta) & \text{for } t > 2, \end{cases}$$

$$\gamma_2(t) = \begin{cases} \bar{\gamma} & \text{for } t \in [0, 1], \\ \bar{\gamma}(1 + \delta) & \text{for } t \in ]1, 2], \\ \bar{\gamma}(1 - \delta) & \text{for } t > 2, \end{cases} \quad \beta_2(t) = \begin{cases} \bar{\beta} & \text{for } t \in [0, 1], \\ \bar{\beta}(1 + \delta) & \text{for } t \in ]1, 2], \\ \bar{\beta}(1 - \delta) & \text{for } t > 2, \end{cases}$$

$$\gamma_3(t) \equiv \bar{\gamma}(1 - \delta), \quad \beta_3(t) \equiv \bar{\beta}(1 - \delta),$$

$$\gamma_4(t) \equiv \bar{\gamma}, \quad \beta_4(t) \equiv \bar{\beta}.$$

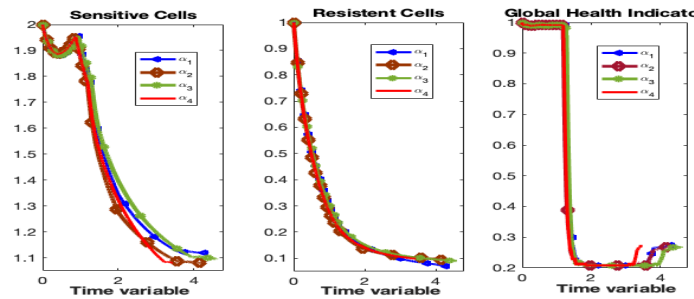


FIGURE 12 (Test 6) - Admissible trajectories corresponding to different uncertainties

We observe in Figure 12 that the overall trajectories are quite similar. However, the time of entry in  $\mathcal{N}_{T_0}$  depends on the outcome of the uncertainties  $\alpha_i$  which confirms that the computed trajectories adjust to the values of the uncertainties  $\alpha$ .

## ACKNOWLEDGEMENT

This work is partially supported by a public grant overseen by the French National Research Agency (ANR) through the "iCODE Institute project" funded by the IDEX Paris-Saclay ANR-11-IDEX-0003-02, and by the DGA under grant 0660037.

## References

1. Ding L, Ley TJ, Larson D, et al. Clonal evolution in relapsed acute myeloid leukaemia revealed by whole-genome sequencing. *Nature* 2012; 481(7382): 506–510.
2. Birkhead B, Gregory W. A mathematical model of the effects of drug resistance in cancer chemotherapy. *Mathematical biosciences* 1984; 72(1): 59–69.
3. Birkhead B, Rankin E, Gallivan S, Dones L, Rubens R. A mathematical model of the development of drug resistant to cancer chemotherapy. *European Journal of Cancer and Clinical Oncology* 1987; 23(9): 1421–1427.
4. Ledzewicz U, Schättler H. Drug resistance in cancer chemotherapy as an optimal control problem. *Discrete and Continuous Dynamical Systems Series B* 2006; 6(1): 129.
5. d’Onofrio A, Ledzewicz U, Maurer H, Schättler H. On optimal delivery of combination therapy for tumors. *Mathematical biosciences* 2009; 222(1): 13–26.
6. Schättler H, Ledzewicz U. *Geometric optimal control: theory, methods and examples*. Vol. 38 of *Interdisciplinary applied mathematics*. Springer-Verlag New York . 2012.
7. Schättler H, Ledzewicz U. *Optimal Control for Mathematical Models of Cancer Therapies*. Vol. 42 of *Interdisciplinary Applied Mathematics*. Springer-Verlag New York . 2015
8. Carrère C. Optimization of an in vitro chemotherapy to avoid resistant tumours. *Journal of Theoretical Biology* 2017; 413: 24–33.
9. Mitchell I, Bayen A, Tomlin C. A time-dependent Hamilton-Jacobi formulation of reachable sets for continuous dynamic games. *IEEE Transactions on automatic control* 2005; 50(7): 947-957.
10. Kurzhanski A, Mitchell IM, Varaiya P. Optimization technics for state constrained control and obstacle problems. *Journal of Optimization, Theory and Applications* 2006; 128(3): 499-521.
11. Margellos K, Lygeros J. Hamilton-Jacobi formulation for Reach-Avoid Problems with an application to Air Traffic Management. In: . Proceedings of the American Control Conference. Proceedings of the American Control Conference. ; 2010; Baltimore, MD, USA.
12. Lygeros J. On reachability and minimum cost optimal control. *Automatica* 2004; 40: 917–927.
13. Kurzhanski A, Varayia P. On reachability under uncertainty. *SIAM J. Control and Optimization* 2002; 41(1): 181-216.
14. Chen M, Herbert S, Tomlin CJ. Fast reachable set approximations via state decoupling disturbances. In: IEEE 55th Conference on Decision and Control (CDC). ; 2016: 191–196
15. Bokanowski O, Forcadel N, Zidani H. Reachability and minimal times for state constrained nonlinear problems without any controllability assumption. *SIAM Journal on Control and Optimization* 2010; 48(7): 4292–4316.
16. Altarovici A, Bokanowski O, Zidani H. A general Hamilton-Jacobi framework for non-linear state-constrained control problems. *ESAIM: Control, Optimisation and Calculus of Variations* 2013; 19(2): 337–357.
17. Desilles A, Zidani H, Crück E. Collision analysis for an UAV. In: Proceedings of AIAA Guidance, Navigation, and Control Conference. ; 2012: 4526.
18. Elliott J, Kalton N. *The existence of value in differential games*. American Mathematical Society, No. 126, Providence . 1972.
19. Clark P, Slevin M, Joel S, et al. A randomized trial of two etoposide schedules in small-cell lung cancer: the influence of pharmacokinetics on efficacy and toxicity.. *Journal of Clinical Oncology* 1994; 12(7): 1427-1435. PMID: 8021734doi: 10.1200/JCO.1994.12.7.1427

20. Barbolosi D, Freyer G, Ciccolini J, Iliadis A. Optimisation de la posologie et des modalités d'administration des agents cytotoxiques à l'aide d'un modèle mathématique. *Bulletin du Cancer* 2003; 90(2): 167–75.
21. Cardaliaguet P. A differential game with two players and one target. *SIAM J. Control and Optimization* 1996; 34(4): 1441–1460.
22. Aubin J. *Viability theory*. Birkhäuser, Boston, MA . 1991.
23. Bardi M, Capuzzo-Dolcetta I. *Optimal control and viscosity solutions of Hamilton-Jacobi-Bellman equations*. Systems and Control: Foundations and Applications Birkhäuser, Boston . 1997.
24. Evans W. *Partial Differential Equations*. American Mathematical Society . 1988.
25. Osher S, Shu CW. High essentially nonoscillatory schemes for Hamilton-Jacobi equations. *SIAM Journal of Numerical Analysis* 1991; 28(4): 907-922.
26. Sethian JA. *Level set methods and fast marching methods*. 3 of *Cambridge Monographs on Applied and Computational Mathematics*. Cambridge: Cambridge University Press. second ed. 1999. Evolving interfaces in computational geometry, fluid mechanics, computer vision, and materials science.
27. Falcone M, Giorgi T, Loreti P. Level sets of viscosity solutions : some applications to fronts and rendez-vous problems. *SIAM J. Applied Mathematics* 1994; 54(5): 1335-1354.
28. Falcone M, Ferretti R. *Semi-Lagrangian approximation schemes for linear and Hamilton-Jacobi equations*. Philadelphia: SIAM . 2014.
29. Sethian JA, Vladimirovsky A. Ordered upwind methods for static Hamilton–Jacobi equations: theory and algorithms. *SIAM Journal on Numerical Analysis* 2003; 41(1): 325–363. doi: doi:10.1137/s0036142901392742
30. Bokanowski O, Falcone M, Ferretti R, Kalise D, Grüne L, Zidani H. Value iteration convergence of  $\epsilon$ -monotone schemes for stationary Hamilton-Jacobi equations. *Discrete and Continuous Dynamical Systems - Serie A* 2015; 35(9): 4041–4070. doi: 10.3934/dcds.2015.35.4041
31. Crandall M, Lions PL. Two approximations of solutions of Hamilton-Jacobi equations. *Mathematics of Computation* 1984; 43(167): 1–19.
32. Bokanowski O, Maroso S, Zidani H. Some convergence results for Howard's algorithm. *SIAM Journal on Numerical Analysis* 2009; 47(4): 3001–3026.
33. Alla A, Falcone M, Kalise D. An efficient policy iteration algorithm for dynamic programming equations. *SIAM J. of Scientific Computing* 2015; 37: 181–200. doi: 10.1137/130932284
34. Assellaou M, Bokanowski O, Désilles A, Zidani H. Value function and optimal trajectories for a maximum running cost control problem with state constraints. Application to an abort landing problem.. *ESAIM: Mathematical Modelling and Numerical Analysis (ESAIM: M2AN)* 2018; 52(1): 305–335.

